ELSEVIER

Contents lists available at ScienceDirect

# Algal Research

journal homepage: www.elsevier.com/locate/algal





# Enhanced carbon capture and polyunsaturated fatty acid production by *Phaeodactylum tricornutum* after stepwise CO<sub>2</sub> acclimation

Shuyu Xie a,b,1, Xin Zhao a,1, Yuan Feng a, Guang Gao a,\*

- a State Key Laboratory of Marine Environmental Science, College of Ocean and Earth Sciences, Xiamen University, Xiamen, 361005, China
- b Key Laboratory of Marine Environmental Survey Technology and Application, Ministry of Natural Resources, Guangzhou, 510301, China

#### ARTICLE INFO

Keywords:
Biofuel
Carbon capture
Diatom
Fatty acid
Flue gas
Lipid

#### ABSTRACT

Industrial flue gas serves as a major source of  $CO_2$  emissions. Currently, the exploration on how to use microalgae to absorb it and produce more lipids and polyunsaturated fatty acids (PUFAs) has emerged as a promising research direction. However, maintaining microalgal growth rates under high  $CO_2$  concentrations remains a key bottleneck in research. In response to this, we pioneered a stepwise  $CO_2$  acclimation approach, whereby *Phaeodactylum tricornutum*—a model diatom isolated from the South China Sea with rapid growth and high PUFA content—were sequentially acclimated to 2 %, 5 % and 7.5 %  $CO_2$ . The results demonstrated that this approach enabled more stable growth. Furthermore, after acclimation, larger cell diameter, more carbon accumulation, higher carbon capture rate and lipid production were attained. The coupling of 7.5 %  $CO_2$  and nitrogen deficiency (HCLN) resulted in 69.1 % higher carbon capture rate at 6 h and induced higher lipid productivity by 32 %, 46 % and 44 % at 6 h, 12 h and 24 h, respectively compared to 0.04 %  $CO_2$  & high nitrogen (ACHN). In addition, the production of PUFAs was also promoted, especially for eicosapentaenoic acid (EPA) and docosahexaenoic acid (DHA). The maximum promoting effect of HCLN on EPA and DHA appeared at 6 h with increases of 64 % and 280 % respectively compared to ACHN. This study suggests that the stepwise  $CO_2$  acclimation strategy is an effective approach for microalgae to capture  $CO_2$  and produce lipid and PUFAs, which is beneficial for the combination of flue gas treatment and product markets (e.g., biofuel and health care).

# 1. Introduction

The increasing concentration of  $CO_2$  in the atmosphere leads to more and more serious climate change and extreme weather, such as global warming, ocean acidification and marine heat waves, which is affecting the economic development and health of human [1,2]. It is well known that the main factors for the increasing  $CO_2$  are the rapid development of heavy industry and the extensive use of fossil fuels [3].  $CO_2$  in flue gas has traditionally been absorbed through chemical and physical, methods, which are effective but costly and ecologically damaging. Microalgae-based biological approaches are a more environmentally friendly and sustainable alternative for flue gas treatment and renewable biofuel production [4]. In addition, in order to reduce  $CO_2$  emission at source, the feasible and effective approach is to replace fossil fuels with carbon-zero bioenergy [5].

As the third-generation biofuel, algae have many advantages compared to the first and second generation, such as faster growth rate,

higher photosynthesis effectivity, without competing for arable land with crops and easy extraction [6-8]. There are a variety of researches on algae suitability for use as biofuels, including macroalgae and microalgae, freshwater and seawater species [9-11]. Among them, Chlorella, Dunaliella, and Nannochloropsis have received much more attention thanks to their high growth rates and lipid content [12,13]. Currently, there is increasing attention to diatom species, which contributes 40 % of the marine's primary productivity [1,14]. In addition to biofuel, lipid produced by microalgae can be an ideal source for generating valuable polyunsaturated fatty acids (PUFA), such as docosahexaenoic acid (DHA) and eicosapentaenoic acid (EPA), which are beneficial for human health [15,16]. It was well known that human cannot synthetize DHA and EPA in vivo, and regular consumption of EPA and DHA supplements has been shown to reduce inflammation and prevent cardiovascular disease [17], so they must depend on food. However, by far the majority of DHA and EPA comes from marine fish oil, which can lead to overfishing. Although more and more attention

E-mail address: guang.gao@xmu.edu.cn (G. Gao).

 $<sup>^{\</sup>star}$  Corresponding author.

 $<sup>^{1}\,</sup>$  These authors contributed equally to this work.

Algal Research 91 (2025) 104298

has been paid to the production of PUFA by diatoms, the understanding on the combination of flue gas treatment and PUFA production with diatom remains limited.

S. Xie et al.

Lipid synthesis in microalgae is often increased under environmental stress, including high CO2 conditions. CO2 assimilation by microalgae serves as a critical determinant for the biosynthesis of cellular lipids and fatty acids. Microalgae absorb CO2 from seawater and concentrate it intracellularly via the CO<sub>2</sub> concentrating mechanism (CCMs) to facilitate carbon fixation. The fixed carbon is subsequently allocated to lipid and fatty acid biosynthesis [18-21]. Consequently, elevated environmental CO2 levels could enhance lipid and fatty acid accumulation in microalgae. For instance, compared to the ambient CO2 (0.04 % CO2), lipid content of Skeletonema costaum was enhanced by 70 % and 87 % at 5 % and 10 % CO<sub>2</sub> concentration, respectively [1]. Lipid productivity of S. costaum was increased by 42.7 % and 113.7 % for 12 h induction under Si-limitation and N-Si-limitation, respectively [7]. Xie et al. demonstrated that carbon removal rate and lipid content of S. costaum were increased by 28.9 % and 26.8 % under 5 % CO<sub>2</sub>, respectively [14]. However, previous studies had promoted lipid the expense of growth rates, although an effective two-stage culture model had been adopted to address this challenge. How to domesticate acid-resistant microalgae to maintain stable growth and promote the accumulation of lipids and fatty acids still faces great challenges.

Currently, the production of biomass from flue gas primarily relies on freshwater algae, with limited research focusing on marine diatoms [4,22]. However, marine diatoms offer distinct advantages for cultivation in coastal regions. Notably, diatoms exhibit remarkable adaptability the intense fluctuations of outdoor light intensity, making them highly suitable for outdoor cultivation. Among marine diatoms, P. tricornutum stands out as a unicellular species capable of accumulating a large amount of EPA, positioning it as a promising candidate for industrial production of EPA [23]. Considering the challenges in maintaining stable growth and promoting the accumulation of lipids and fatty acids in high CO2 conditions for marine diatoms, this study pioneered a stepwise CO<sub>2</sub> domestication approach to culture P. tricornutum. The primary objectives were to evaluate its potential for CO<sub>2</sub> capture and its capacity for polyunsaturated fatty acid (PUFA) production. This work aims to bridge the gap in understanding the applicability of marine diatoms for both environmental remediation and high-value compound synthesis. Specifically, it focuses on answering a critical question: How can marine diatoms acclimate to high CO2 environments and simultaneously achieve the dual goals of rapid CO2 removal and high PUFA production? The rapid societal development has brought increasing challenges in balancing economic growth with environmental protection, particularly in managing industrial emissions. This study addresses these dual challenges by developing an eco-efficient system for (1) flue gas reutilization remediation through microalgal cultivation and (2) concurrent production of lipid-based biofuels. Our study demonstrates how carbon capture and utilization (CCU) technologies can transform industrial exhaust streams into valuable bioenergy resources, offering a sustainable pathway for China's carbon neutrality initiatives.

### 2. Materials and methods

#### 2.1. Algae culture and experimental design

The strain of *Phaeodactylum tricornutum* was Pt11 (CCMA106), isolated and purified from the South China Sea, China. The cells exhibited a typical fusiform shape, with a length of 12–16  $\mu$ m and a width of 3–4  $\mu$ m (Supplementary Fig. 1). They were cultured in 500 mL PC bottles at 20 °C with sterilized artificial seawater, and the light intensity was set at 100  $\mu$ mol photons m<sup>-2</sup> s<sup>-1</sup> (light: dark = 16: 8) using an incubator (HP200G-3 light incubator, Ruihua, Wuhan, China). The f/2 medium was supplemented into sterilized artificial seawater, resulting in final concentration of 882.35  $\mu$ mol L<sup>-1</sup> nitrate (NO<sub>3</sub>) and 36.23 phosphate (PO<sub>4</sub><sup>3</sup>–) in the algal culture medium. The cells were diluted every 4 days

by semi-continuous culture, and the initial concentration of cells was maintained at 200  $\times$   $10^4$  cell  $mL^{-1}.$ 

 $CO_2$  concentration in flue gases can range from 3 % to 15 % [24,25]. In this study, we aimed to culture P. tricornutum under 7.5 % CO<sub>2</sub>. A stepwise domestication approach was employed since cells were unable to grow when they were cultured under 7.5 % CO2 directly (Supplementary Fig. 2). Cells were at 2 %, 5 % and 7.5 % CO<sub>2</sub> sequentially. P. tricornutum was first cultured in 2 % CO<sub>2</sub> for 16 days, and then in 5 % CO<sub>2</sub> for 138 days to adapt the high CO<sub>2</sub> concentration. Finally, the cells were transferred to 7.5 % CO<sub>2</sub> concentration and cultured for 24 days. To induce more lipid and PUFA, a high CO2 (7.5 %) combined with nitrogen deficiency (0  $\mu$ mol L<sup>-1</sup>) experiment was carried out. Cells were cultured in four conditions: ambient CO2 & high N (ACHN), ambient CO2 & low N (ACLN), high CO2 & high N (HCHN), high CO2 & low N (HCLN) respectively. The high N concentration was 882.35  $\mu$ mol L<sup>-1</sup>. ACHN was set as the control in this experiment. All experiments were conducted in triplicate. The CO<sub>2</sub> concentrations of control (0.04 % CO<sub>2</sub>, AC) and treatment (2 % CO2, 5 % CO2, 7.5 % CO2, HC) groups were maintained by bubbling outdoor air and/or CO2 enricher (CE100C-2, Ruihua, Wuhan, China), and the ventilated gases were filtered through a 0.2 µm HEPA filter membrane with an aeration rate of 500 mL/min, controlled by a flowmeter.

#### 2.2. Measurement of carbonate chemistry

The pH and total alkalinity (TA) were measured before the dilution. Ten mL of algal solution was taken for pH using a pH meter (310P-01 A, Thermo Fisher, USA), and the pH meter was calibrated using NBS buffer prior to sample determination. An automated system (AS-ALK2, APOLLO SCITECH, USA) was used to measure TA. The pH was measured every day during the  $\rm CO_2$  acclimation experiment (2 %, 5 % and 7.5 %  $\rm CO_2$ ). Since daily variations in pH was minimal, only day 4 data were presented. As for the experiment of 7.5 %  $\rm CO_2$  & N deficiency, the samples were measured at 6 h, 12 h and 24 h. Known values of pH and TA were used to derive the dissolved inorganic carbon (DIC),  $\rm HCO_3^-$ ,  $\rm CO_3^-$  and dissolved  $\rm CO_2$  ( $\rm CO_{2aq}$ ) using CO2SYS (Supplementary Table 1&2).

#### 2.3. Measurement of growth rate and cell diameter

Z-2TM Coulter (Z2, Backman Coulter, USA) was used to measure the cell concentrations and diameter before and after dilution. The specific growth rate (SGR) was calculated by the equation [14]:

$$SGR = \frac{\ln(N_n/N_0)}{t_n - t_0} \tag{1}$$

where  $N_n$  and  $N_0$  represent the cell numbers at time  $t_n$  and  $t_0$ , respectively. The cell diameter was read directly by Z-2TM Coulter.

### 2.4. Measurement of photochemical performances

The photosynthetic parameters, including the maximum photochemical efficiency (Fv/Fm) of photosystem II and the non-photochemical quenching (NPQ), were determined by multi-excitation wavelength chlorophyll fluorescence analyzer (XE-PAM, Walz, Effeltrich, Germany) after dark adaptation for 15 mins. The saturation pulse was set to 5000  $\mu$ mol photons m $^{-2}$ s $^{-1}$ , and the actinic light was set the same as culture light intensity, Fv/Fm and NPQ were calculated according to the following formula [26,27]:

$$Fv / Fm = \frac{F_m - F_0}{F_m} \tag{2}$$

$$NPQ = \frac{F_m - F_m}{F_m} \tag{3}$$

where  $F_m$  and  $F_0$  are maximum and minimum chlorophyll fluorescence of cells after 15 mins dark adaptation, respectively, and Fm' is the maximum fluorescence yield under actinic light.

#### 2.5. Measurement of photosynthetic pigments

Fresh cells were filtered onto GF/F membrane (Whatman, 25 mm) within a pressure of 0.02 MPa, extracted with 5 mL methanol (100 %) under 4  $^{\circ}$ C overnight, and centrifuged at 8000g for 10 mins. The supernatant was measured using a spectrophotometer (TU-1810DASPC, Persee, China). And then, the chlorophyll a (Chl a) and carotenoid were calculated according the following equations [28]:

Chl a 
$$(pg \ cell^{-1}) = 13.2654 \times (A_{665} - A_{750}) - 2.6839 \times (A_{632} - A_{750})$$
(4)

$$Car\left(pg\ cell^{-1}\right) = 7.6 \times \left[\left(A_{480} - A_{750}\right) - 1.49 \times \left(A_{510} - A_{750}\right)\right]$$
 (5)

where  $A_{480}$ ,  $A_{510}$ ,  $A_{632}$ ,  $A_{665}$ , and  $A_{750}$  represent the absorbances of the methanol extracts at 480, 510, 632, 665, and 750 nm respectively.

# 2.6. Measurement of particular organic carbon (POC) and carbon capture rate

POC sample was harvested onto GF/F membrane (Whatman, 25 mm), which was pre-burned by muffle furnace with 450 °C for 4 h, and then stored at -20 °C. Before determination, samples were fumigated with HCl (12 mol L $^{-1}$ ) for 24 h to remove inorganic carbon, and then dried in an oven (DHG-9146 A, Jing Hong, China) for another 24 h. POC were then measured with the Elementar Vario EL Cube (Elementar, Germany).

Based on POC and cell concentrations, carbon capture rate was calculated, and the formula was as follows [14]:

Carbon capture rate 
$$(pg cell^{-1}d^{-1}) = \frac{(C_t \times POC_t - C_0 \times POC_0)}{C_0} \times t$$
 (6)

where  $C_t$  and  $C_0$  represent the cell concentrations after culture (t) and the initial cell concentration, respectively. Similarly,  $POC_t$  and  $POC_0$  represent the POC content after culture (t) and the initial POC content, respectively.

# 2.7. Measurement of total lipid and lipid productivity

At the time of sampling, a quantitative volume of algal solution was

lower layer of chloroform layer was taken into a glass tube with a Pasteur pipette, and then blown to dryness using a nitrogen blowing machine (NDK200-1 N, MIULAB, China), then weighed, and the percentage of the lipid content, total lipid content, and lipid content of the algal powder was calculated. The percentage of total lipid content and lipid productivity were calculated as follows [7]:

$$Lipid (\%DW) = \frac{m_1}{m_a} \tag{7}$$

$$\textit{Lipid productivity } (pg/cell/d) = \frac{m_t \times C_t/C_t \times V_t - m_0 \times C_0/C_0 \times V_0}{C_0 \times t} \times 10^9$$
 (8)

where  $m_l$ ,  $m_a$ ,  $m_t$  and  $m_0$  represent the weight of lipid extracted, algae powder, lipid extracted from the sample at incubation time and initial weight of lipid extracted from the sample, respectively.  $C_t$  and  $C_0$  represent the cell concentration at incubation time t and the beginning time, respectively.  $V_t$  and  $V_0$  represent the sampling volume at incubation time t and initial sampling volume, respectively. The incubation time was t (h or d).

#### 2.8. Measurement of fatty acid and fatty acid productivity

The extracted total lipid samples were methylated with fatty acids, 2 mL of sulfuric acid-methanol solution (v:v = 2.0 %) was added, the centrifuge tube was capped with 20 s of nitrogen, and the samples were mixed with a multitube vortex mixer (2000 rpm, 10 mins), heated in a water bath at 80 °C for 1 h, and then 1 mL of saturated sodium chloride solution and 2 mL of n-hexane were added and mixed (2000 rpm, 10 mins). After centrifugation (3000 g, 5 mins), the supernatant was filtered through 0.22 µm organic filter membrane into the injection bottle, and stored at -20 °C under the condition of light protection. The online determination of fatty acids was carried out by a gas chromatograph Agilent 5977B (Agilent, USA) with a 10 µL injection, and analysed on an Agilent HP-5 (30 m  $\times$  0.25 mm  $\times$  0.25  $\mu$ m) chromatographic column (Agilent, USA). Purified helium was used as the carrier gas with a total flow rate of 15.1 mL/min, a purge flow rate of 3 mL/min, an inlet temperature of 260 °C, a split ratio set at 10:1 and a split flow rate of 11 mL/min. Fatty acid contents and yields were calculated according to the following equations [7]:

$$FA (\mu g/mg DW) = \frac{FA_t \times V/V_t}{m_0/V_t}$$
(9)

FA productivity 
$$(fg/cell/h) = \frac{FA_t \times V/(C_t \times V_t) \times C_t - FA_0 \times V/(C_0 \times V_0) \times C_0}{C_0 \times t} \times 10^9$$
 (10)

filtered onto a 0.12  $\mu m$  PC membrane and stored at -20 °C. The cells were rinsed from the membrane samples into centrifuge tubes using artificial seawater before the assay, and the supernatant was removed by centrifugation (8960 g, 10 mins, 4 °C) and dried in an oven at 60 °C to make algal powder. Algae powder was weighed, and 6 mL of chloroform-methanol solution (v:v = 2:1) and 1 mL of NaCl solution (0.88 %) were added to each sample of algal powder, which was mixed with a multi-tube vortex mixer (DMT-2500, China) at 2000 rpm for 20 mins, and after mixing, centrifugation (8960 g, 10 mins, 4 °C) was performed to remove the supernatant, and 6 mL of methanol-water solution (v:v = 2:1) was added. The supernatant was removed, and then 6 mL of methanol-water solution (v:v = 1:1) was added to the supernatant (2000 rpm, 20 min), and centrifuged again (8960 g, 10 min, 4 °C). The

where  $FA_t$  and  $FA_0$  represent the fatty acid content at induction time t and initial fatty acid content, respectively.  $V_t$ ,  $V_0$  and V represent the sampling volume at induction time t and initial and the fatty acid sample volume, respectively. The weight of algal powder at induction time was represented by  $m_a$ , and the concentration of cells at the initial was represented by  $C_0$ . The incubation time was t (h).

#### 2.9. Statistical analysis

The data in this study was all expressed by the mean  $\pm$  sd and statistical analysis was performed using SPSS 26 and/or R language (version 4.3.1). The data conformed to a normal distribution (Shapiro-

Wilk, p>0.05) and the variances could be considered equal (Levene's test, p>0.05). For high CO<sub>2</sub> experiment, one-way ANOVA and generalized additive models (GAMs) were used to analysis the significance of difference between different treatments and the patterns of parameters over time. For 7.5 % CO<sub>2</sub> & N limitation experiment, the three-factor analysis of variance was used to determine whether there was an interaction between the three factors (CO<sub>2</sub>, nitrogen and time), and then LSD was used for post hoc comparisons by SPSS 26.

#### 3. Results

#### 3.1. Carbonate chemistry

As shown in Supplementary Table 1, HC significantly decreased pH and  $\text{CO}_{2}^{3-}$ , and significantly increased DIC,  $\text{HCO}_{3}^{-}$  and  $\text{CO}_{2aq}$  at each  $\text{CO}_{2}$  concentration. For instance, pH was reduced by 3.1, 3.4 and 3.7 by 2 %  $\text{CO}_{2}$ , 5 %  $\text{CO}_{2}$ , and 7.5 %  $\text{CO}_{2}$  concentration, respectively. In addition, high  $\text{CO}_{2}$  concentration significantly increased the concentrations of DIC and  $\text{HCO}_{3}^{-}$  by 245 %–393 % and 1188 %–1915 %, respectively. The  $\text{CO}_{2aq}$  concentration of AC was almost zero (0.02–0.06  $\mu\text{M}$ ), whereas the range of HC was 530–1910  $\mu\text{M}$ . However, the TA was stable under high  $\text{CO}_{2}$  concentration except for 7.5 %  $\text{CO}_{2}$ . For the two-factor experiment (7.5 %  $\text{CO}_{2}$  & N limitation), the variation trend of the parameters of the seawater carbonate system was similar to that of the high-CO $_{2}$  experiment, as shown in the Supplementary Table 2.

#### 3.2. Specific growth rate at different CO<sub>2</sub> concentrations

Different effects were shown at different  $\mathrm{CO}_2$  concentration on growth. At 2 % concentration, the specific growth rate (SGR) was always higher than that of AC, especially on the 8th and 16th days, with a significant increase of 19.6 % (ANOVA, p < 0.05) and 10.6 % (ANOVA, p < 0.05), respectively (Fig. 1A). However, when the  $\mathrm{CO}_2$  concentration

increased to 5 %, its effect fluctuated with culture time (Fig. 1B). Differently, there was no significant effects for 7.5 %  $\rm CO_2$  concentration (ANOVA, p>0.05) on growth (Fig. 1C). Based on the analysis of generalized additive models (GAMs), the stimulative effect 2 %  $\rm CO_2$  reached the peak during middle of culture period and then decreased with time. In contrast, the negative effect reached the maximum around day 90 and then returned to neutral by day 130. In terms of 7.5 %  $\rm CO_2$ , although its positive effect seems decreasing with time, this trend was not statistically significant (p=0.559) during the culture period (Fig. 1F).

#### 3.3. Cell diameter at different CO2 concentrations

Cell diameter was all increased at high CO<sub>2</sub> concentrations on average, but the degree of promotion was different (Fig. 2A-C). At the three CO<sub>2</sub> concentrations, the cell diameter of *P. tricornutum* was 4.5 (2 % CO<sub>2</sub>), 5.2 (5 % CO<sub>2</sub>) and 5.6 (7.5 % CO<sub>2</sub>)  $\mu m$  on average, and was promoted by 3.8 %, 22.0 % and 32.0 %, respectively. GAMs indicated that the three CO<sub>2</sub> concentrations significantly promoted the cell diameter during culture (all p<0.05). In the initial stage of 2 % CO<sub>2</sub> culture (Days 0–2), the cell diameter was significantly decreased by about 0.5  $\mu m$ , and then gradually increased, but the increase was always within 0.5  $\mu m$  (Fig. 2D). The range of cell diameter increased at 5 % CO<sub>2</sub> (0–1.5  $\mu m$ , Fig. 2E) was wider than that at 7.5 % CO<sub>2</sub> (1–1.5  $\mu m$ , Fig. 2F) during the whole culture period.

#### 3.4. Fv/Fm at different CO2 concentrations

At 2 % CO $_2$  concentration, the Fv/Fm of *P. tricornutum* was reduced by 2.7 % (ANOVA, p < 0.05), 4.1 % (ANOVA, p < 0.05), and 6.6 % (ANOVA, p < 0.05) on days 0, 4, and 16, respectively (Fig. 3A), and the average reduction was 3.6 %. When CO $_2$  concentration rose to 5 %, the average inhibition rate was 7.0 %, higher than 2 % CO $_2$ , and the

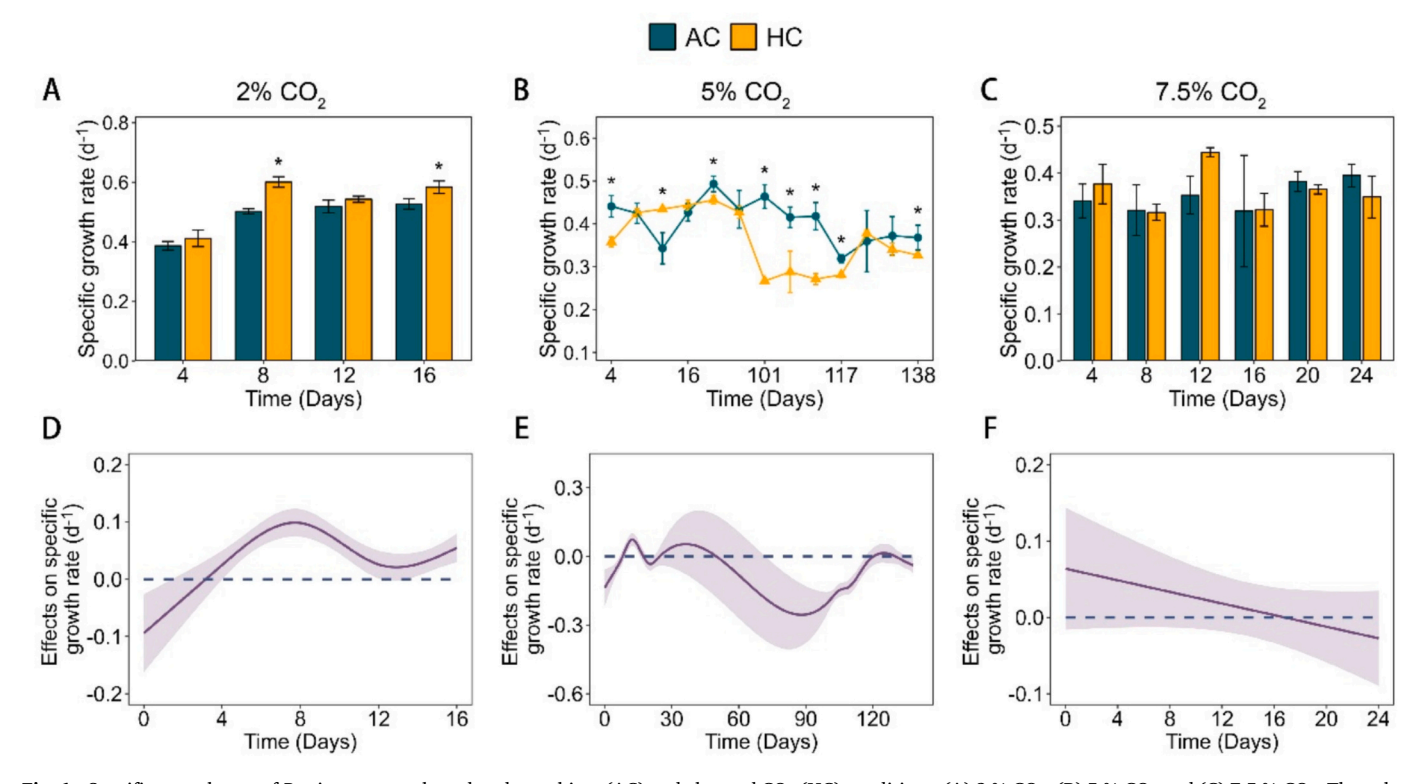


**Fig. 1.** Specific growth rate of *P. tricornutum* cultured under ambient (AC) and elevated  $CO_2$  (HC) conditions. (A) 2 %  $CO_2$ , (B) 5 %  $CO_2$  and (C) 7.5 %  $CO_2$ . The value is mean  $\pm$  standard deviation (SD), and \* indicates that there is a significant difference between the HC and AC (p < 0.05). Effects of 2 %  $CO_2$  (D), 5 %  $CO_2$  (E) and 7.5 %  $CO_2$  (F) on specific growth rate of *P. tricornutum* based on GAMs analysis. Solid lines and shadows are predicted values with 95 % confidence intervals, and the significant differences between the HC and AC are justified by the intersection lack of 95 % confidence intervals and the x-axis.

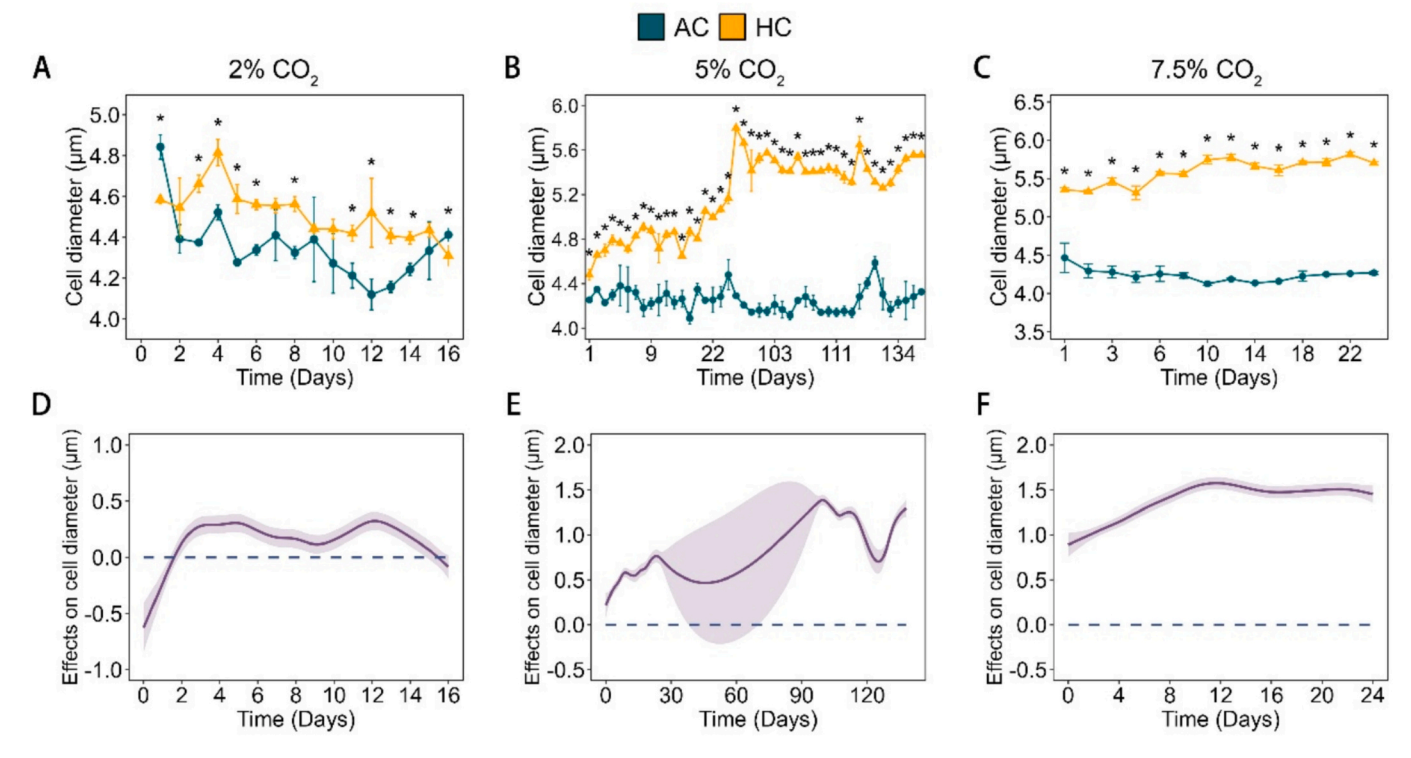


**Fig. 2.** Cell diameter of *P. tricornutum* cultured under ambient (AC) and elevated  $CO_2$  (HC) conditions. (A) 2 %  $CO_2$ , (B) 5 %  $CO_2$  and (C) 7.5 %  $CO_2$ . The value is mean  $\pm$  standard deviation (SD), and \* indicates that there is a significant difference between the HC and AC (p < 0.05). Effects of 2 %  $CO_2$  (D), 5 %  $CO_2$  (E) and 7.5 %  $CO_2$  (F) on cell diameter of *P. tricornutum* based on GAMs analysis. Solid lines and shadows are predicted values with 95 % confidence intervals, and the significant differences between the HC and AC are justified by the intersection lack of 95 % confidence intervals and the x-axis.

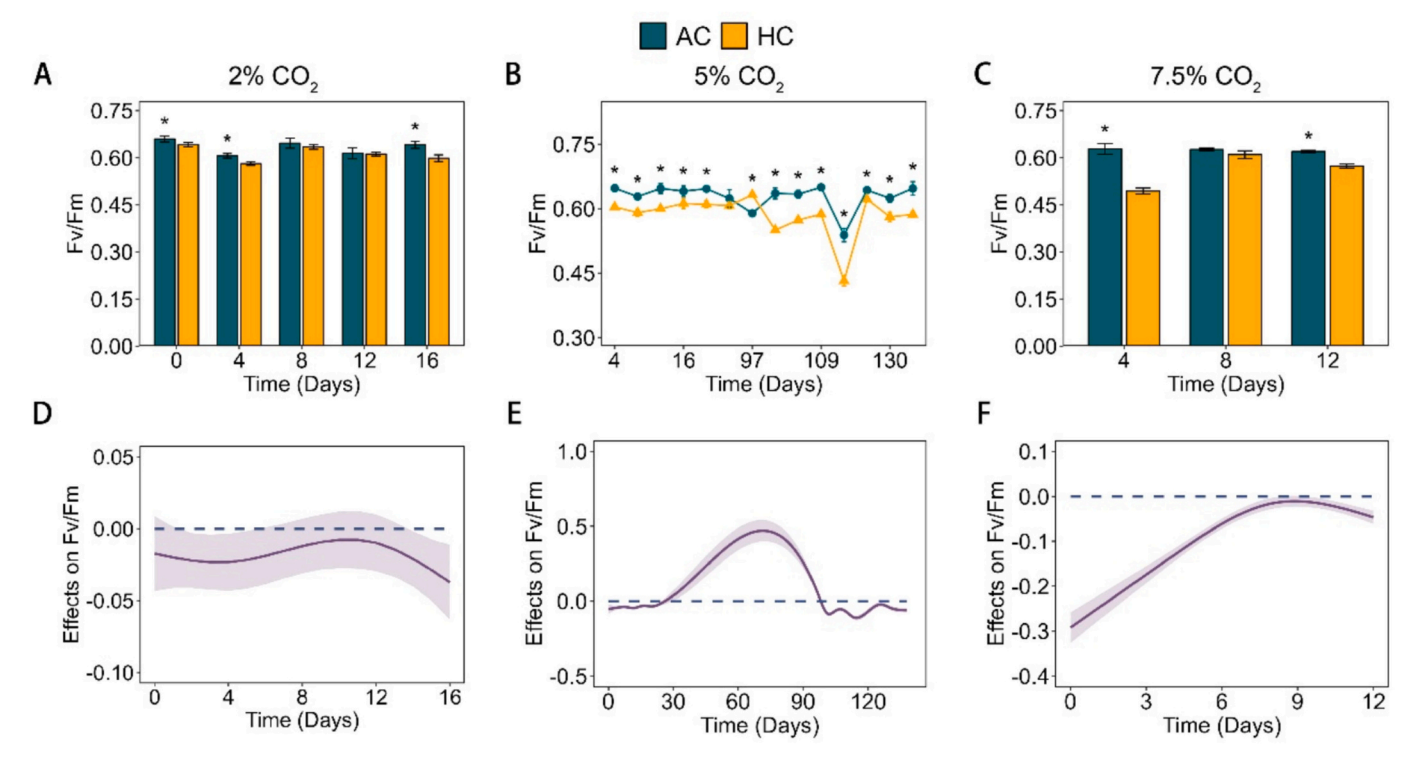


Fig. 3. Fv/Fm of *P. tricornutum* cultured under ambient (AC) and elevated CO<sub>2</sub> (HC) conditions. (A) 2 % CO<sub>2</sub>, (B) 5 % CO<sub>2</sub> and (C) 7.5 % CO<sub>2</sub>. The value is mean  $\pm$  standard deviation (SD), and \* indicates that there is a significant difference between the HC and AC (p < 0.05). Effects of 2 % CO<sub>2</sub> (D), 5 % CO<sub>2</sub> (E) and 7.5 % CO<sub>2</sub> (F) on Fv/Fm of *P. tricornutum* based on GAMs analysis. Solid lines and shadows are predicted values with 95 % confidence intervals, and the significant differences between the HC and AC are justified by the intersection lack of 95 % confidence intervals and the x-axis.

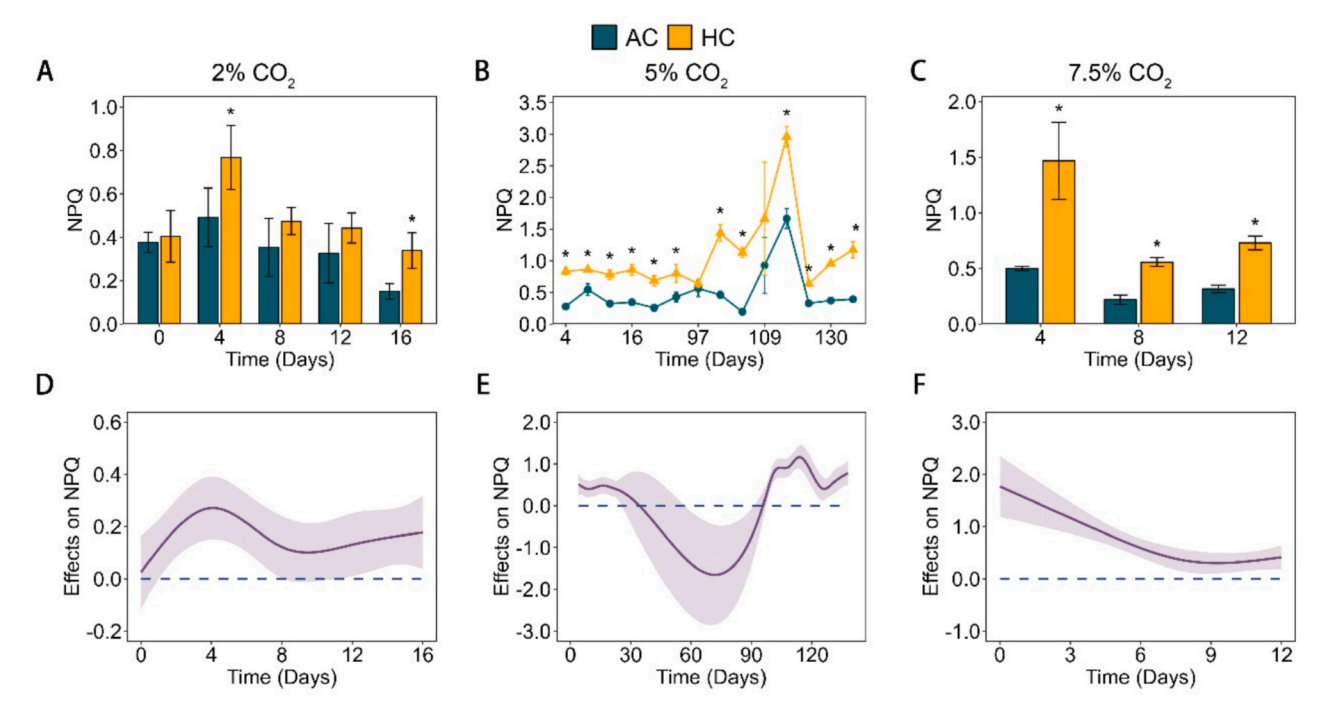
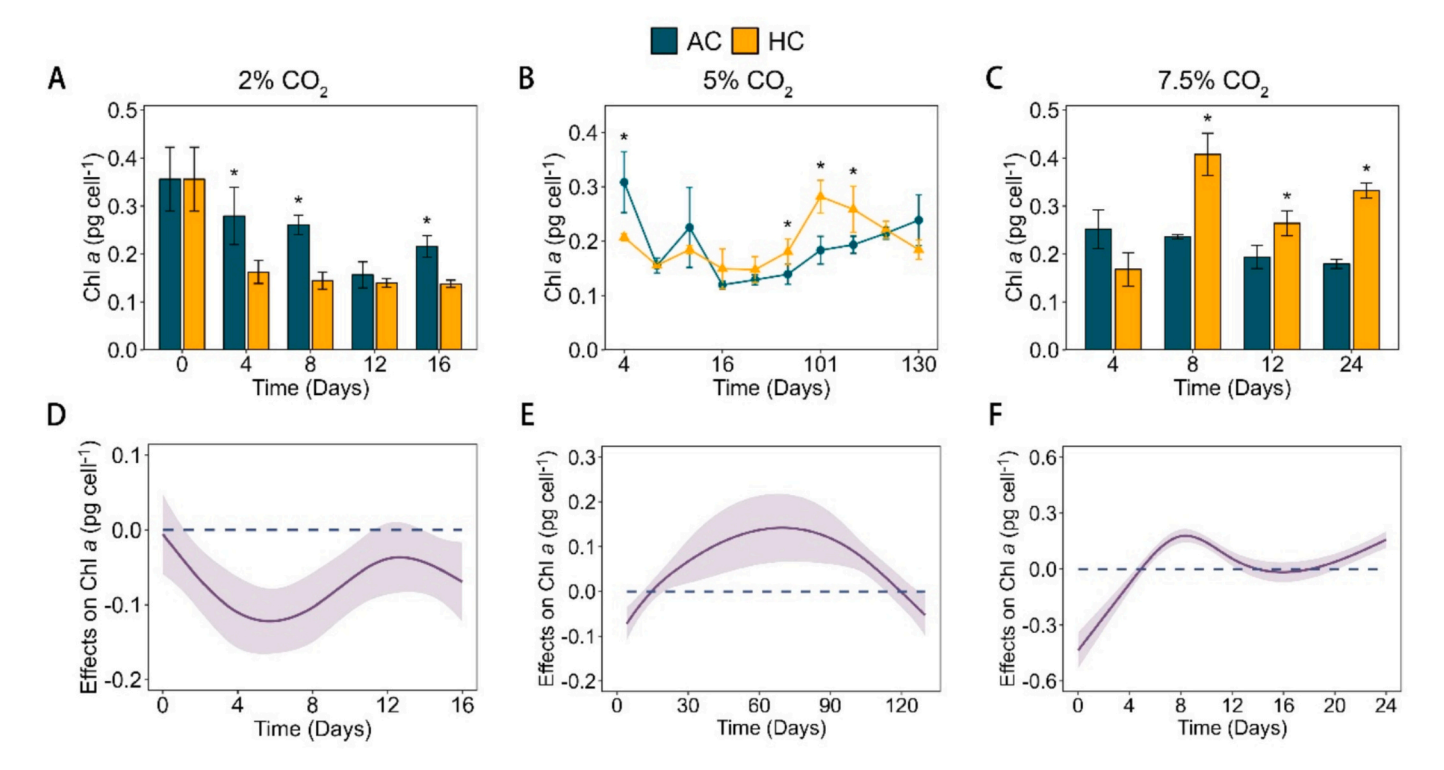


Fig. 4. NPQ of *P. tricornutum* cultured under ambient (AC) and elevated  $CO_2$  (HC) conditions. (A) 2 %  $CO_2$ , (B) 5 %  $CO_2$  and (C) 7.5 %  $CO_2$ . The value is mean  $\pm$  standard deviation (SD), and \* indicates that there is a significant difference between the HC and AC (p < 0.05). Effects of 2 %  $CO_2$  (D), 5 %  $CO_2$  (E) and 7.5 %  $CO_2$  (F) on NPQ of *P. tricornutum* based on GAMs analysis. Solid lines and shadows are predicted values with 95 % confidence intervals, and the significant differences between the HC and AC are justified by the intersection lack of 95 % confidence intervals and the x-axis.

maximum reduction was 19.8 % on day 113 (Fig. 3B). At 7.5 %  $\rm CO_2$  concentration, Fv/Fm was significantly reduced by 21.3 % (ANOVA, p < 0.05) and 7.4 % (ANOVA, p < 0.05) on day 4 and day 12, respectively, with an average reduction of 10.5 % (Fig. 3C), which was the largest

reduction among the three  $\rm CO_2$  concentrations. According to GAMs analysis, Fv/Fm at all three  $\rm CO_2$  concentrations was reduced during the whole culture period except for the middle stage of culture at 5 %  $\rm CO_2$  concentration, but the range and trend of reduction were different. The



**Fig. 5.** Chl a content of P. tricornutum cultured under ambient (AC) and elevated CO<sub>2</sub> (HC) conditions. (A) 2 % CO<sub>2</sub>, (B) 5 % CO<sub>2</sub> and (C) 7.5 % CO<sub>2</sub>. The value is mean  $\pm$  standard deviation (SD), and  $\pm$  indicates that there is a significant difference between the HC and AC (p < 0.05). Effects of 2 % CO<sub>2</sub> (D), 5 % CO<sub>2</sub> (E) and 7.5 % CO<sub>2</sub> (F) on Chl a content of P. tricornutum based on GAMs analysis. Solid lines and shadows are predicted values with 95 % confidence intervals, and the significant differences between the HC and AC are justified by the intersection lack of 95 % confidence intervals and the x-axis.

negative effect at 2 % and 5 %  $\rm CO_2$  was less than that at 7.5 %  $\rm CO_2$  concentration, and the negative effect was weakened at 7.5 %  $\rm CO_2$  (from 0.3 to 0) with the extension of culture time (Fig. 3D-F).

#### 3.5. NPQ at different CO2 concentrations

As depicted in Fig. 4, NPQ of *P. tricornutum* exhibited an increase under all three CO<sub>2</sub> concentrations. Moreover, the degree of increase was found grow with the rise in CO<sub>2</sub> concentration. For example, the increase in NPQ ranged from 7.3 % to 125.3 % under 2 % CO<sub>2</sub> (Fig. 4A), 14.0 %–480.6 % under 5 % CO<sub>2</sub> (Fig. 4B), and 130.5 %–193.5 % under 7.5 % CO<sub>2</sub> (Fig. 4C). Based on GAMs analysis, the promoting effect of 2 % CO<sub>2</sub> presented a trend of initially increasing and then decreasing (Fig. 4D). In contrast, the promoting effect of 5 % CO<sub>2</sub> showed a trend of first decreasing and then increasing. (Fig. 4E). Moreover, the positive effect of 7.5 % CO<sub>2</sub> weakened with the extension of culture time (from 2.0 to nearly 0, Fig. 4F).

#### 3.6. Chl a content at different CO2 concentrations

The 2 % CO<sub>2</sub> had a negative effect on Chl a of P. tricornutum, especially on days 4, 8 and 16, which decreased significantly by 41.8 %, 44.4 % and 36.2 %, respectively (ANOVA, all p < 0.05, Fig. 5A). However, the negative effect gradually weakened at 5 % CO<sub>2</sub> concentration and began to transform into a positive effect by day 16, with a maximum increase of 54.0 % on the 101st day (Fig. 5B). With the increase of CO<sub>2</sub> concentration to 7.5 %, the positive effect of CO<sub>2</sub> on Chl a of P. tricornutum became more and more significant, promoting 36.5 %–85.0 % on days 8 to 24 (Fig. 5C). GAMs analysis revealed concentration-dependent temporal dynamics in CO<sub>2</sub> effects (Fig. 5D-F). The 2 % CO<sub>2</sub> treatment exhibited a triphasic inhibitory pattern: an initial augmentation phase (days 0–8), followed by progressive attenuation (days 8–12), and terminating with a marginal resurgence (Fig. 5D). In contrast, 5 % CO<sub>2</sub> displayed a biphasic response: its initial mild suppression transitioned into a stimulatory effect that escalated progressively, reaching peak

efficacy by day 60 before declining thereafter (Fig. 5E). The negative effect of 7.5 % CO<sub>2</sub> decreased with the extension of culture time and changed to a positive effect after day 4 (Fig. 5F).

#### 3.7. Carotenoid content at different CO<sub>2</sub> concentrations

As shown in Fig. 6A, the response of carotenoid content to 2 % CO<sub>2</sub> concentration was similar to that of Chl a, with an average inhibition rate of 34.2 %. In the first 12 days of culture at 5 % CO<sub>2</sub> concentration, carotenoid content was significantly reduced by 32.4 %, 25.7 % and 28.6 % on days 4, 8 and 12 (ANOVA, all p < 0.05) respectively, after which this negative effect was insignificant until day 130 (23.2 % reduction, ANOVA, p < 0.05, Fig. 6B). When the CO<sub>2</sub> concentration was increased to 7.5 %, the negative effect of CO<sub>2</sub> was still significant on the 4th day (ANOVA, p < 0.05), but changed to a positive effect after the 8th day, with significant increases of 87.1 %, 60.1 % and 53.0 %, respectively (ANOVA, all p < 0.05), on the days 8, 12 and 24 (Fig. 6C). Based on GAMs analysis, the variation trends of carotenoid content of P. tricornutum cultured under three CO<sub>2</sub> concentrations over time were similar to that of Chl a (Fig. 6D-F).

# 3.8. Particulate organic carbon (POC) content at different $CO_2$ concentrations

On days 4 and 12, POC content was significantly increased by 24.9 % and 30.6 % (ANOVA, all p < 0.05), however, it was significantly reduced by 19.0 % on day 16 under 2 % CO<sub>2</sub> concentration (ANOVA, p < 0.05, Fig. 7A). In addition, the POC content was always significantly promoted (ANOVA, all p < 0.05), ranging from 24.2 % to 247.4 %, with an average of 85.5 %, throughout the 138 days' culture period at 5 % CO<sub>2</sub> concentration (Fig. 7B). And then, the promotion effect reached 112.4 % on average, which between 93.0 % to 120.1 % at 7.5 % CO<sub>2</sub> concentration (ANOVA, all p < 0.05, Fig. 7C). GAMs analysis showed that the promoting effect of 2 % CO<sub>2</sub> fluctuated with culture time (p < 0.05, Fig. 7D). The promotion degree of 5 % CO<sub>2</sub> on POC was stronger than 2 % CO<sub>2</sub>,

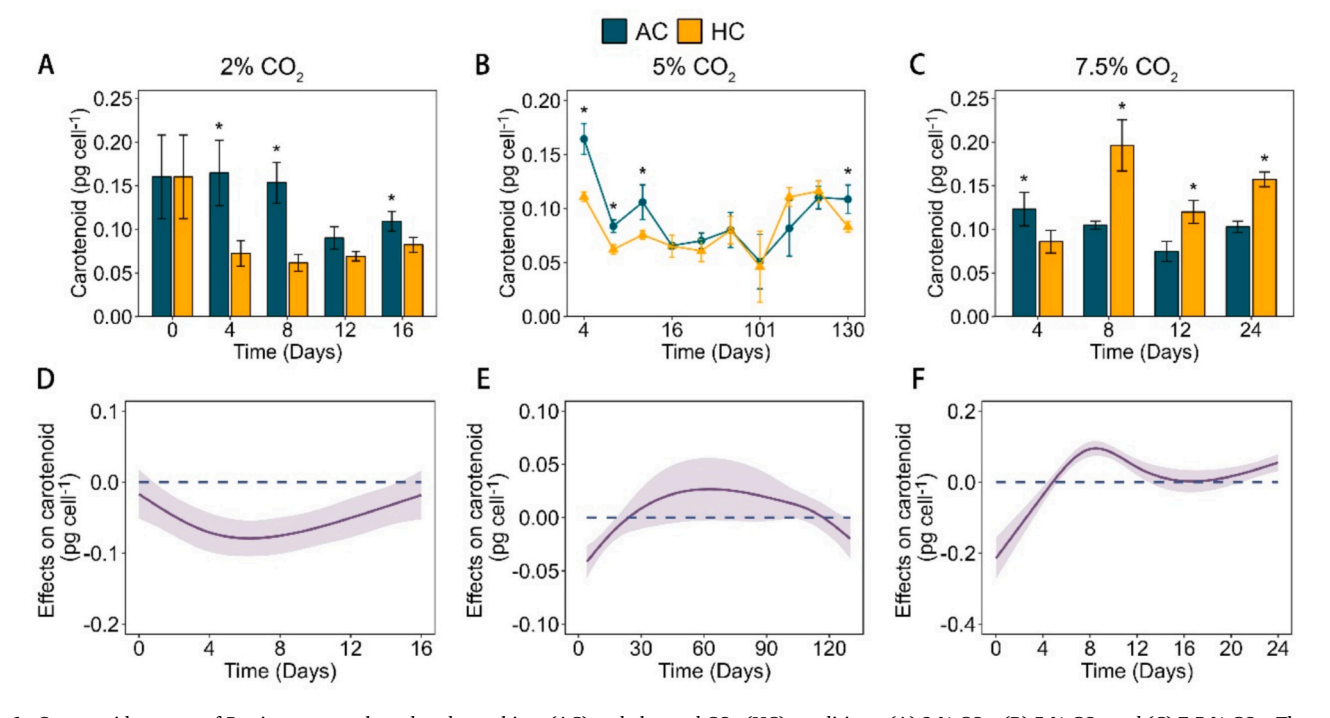


**Fig. 6.** Carotenoid content of *P. tricornutum* cultured under ambient (AC) and elevated  $CO_2$  (HC) conditions. (A) 2 %  $CO_2$ , (B) 5 %  $CO_2$  and (C) 7.5 %  $CO_2$ . The value is mean  $\pm$  standard deviation (SD), and \* indicates that there is a significant difference between the HC and AC (p < 0.05). Effects of 2 %  $CO_2$  (D), 5 %  $CO_2$  (E) and 7.5 %  $CO_2$  (F) on carotenoid content of *P. tricornutum* based on GAMs analysis. Solid lines and shadows are predicted values with 95 % confidence intervals, and the significant differences between the HC and AC are justified by the intersection lack of 95 % confidence intervals and the x-axis.

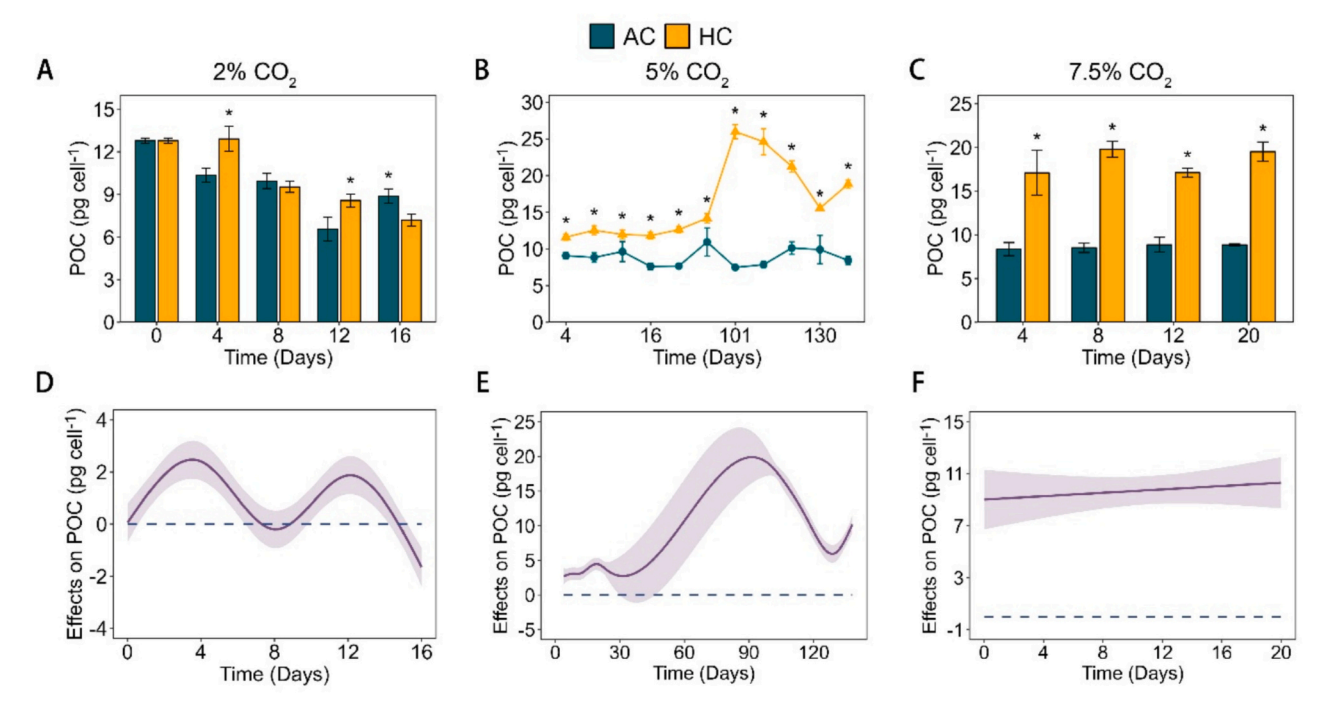


**Fig. 7.** POC content of *P. tricornutum* cultured under ambient (AC) and elevated  $CO_2$  (HC) conditions. (A)  $2\% CO_2$ , (B)  $5\% CO_2$  and (C)  $7.5\% CO_2$ . The value is mean  $\pm$  standard deviation (SD), and \* indicates that there is a significant difference between the HC and AC (p < 0.05). Effects of  $2\% CO_2$  (D),  $5\% CO_2$  (E) and  $7.5\% CO_2$  (F) on POC content of *P. tricornutum* based on GAMs analysis. Solid lines and shadows are predicted values with 95 % confidence intervals, and the significant differences between the HC and AC are justified by the intersection lack of 95 % confidence intervals and the x-axis.

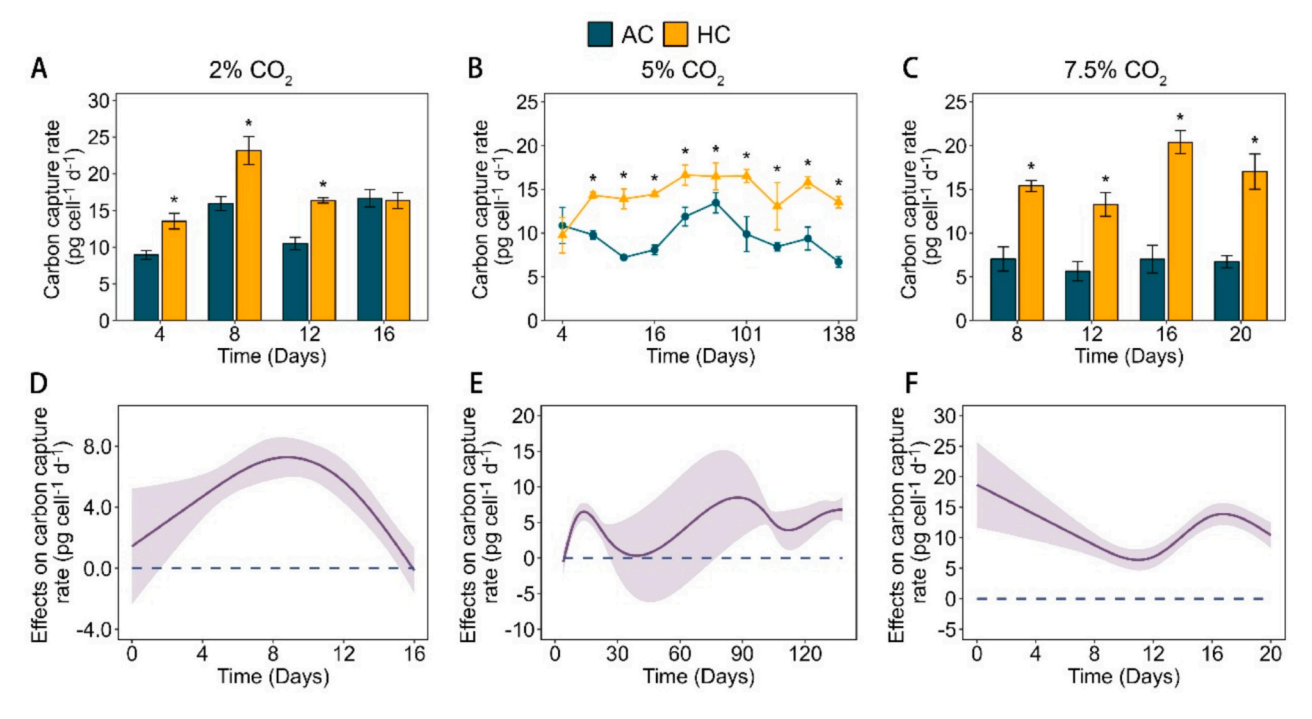


**Fig. 8.** Carbon capture rate of *P. tricornutum* cultured under ambient (AC) and elevated  $CO_2$  (HC) conditions. (A) 2 %  $CO_2$ , (B) 5 %  $CO_2$  and (C) 7.5 %  $CO_2$ . The value is mean  $\pm$  standard deviation (SD), and \* indicates that there is a significant difference between the HC and AC (p < 0.05). Effects of 2 %  $CO_2$  (D), 5 %  $CO_2$  (E) and 7.5 %  $CO_2$  (F) on carbon capture rate of *P. tricornutum* based on GAMs analysis. Solid lines and shadows are predicted values with 95 % confidence intervals, and the significant differences between the HC and AC are justified by the intersection lack of 95 % confidence intervals and the x-axis.

from about 2.5 pg cell $^{-1}$  on day 0 to about 20 pg cell $^{-1}$  on day 90, and then it decreased (p < 0.05, Fig. 7E). Moreover, the promoting effect of 7.5 % CO<sub>2</sub> on POC was more gradual than that of 5 % CO<sub>2</sub>, ranging between 7 and 11 pg cell $^{-1}$  during the 24-day culture period (p < 0.05, Fig. 7F).

### 3.9. Carbon capture rate at different CO2 concentrations

As shown in Fig. 8, the carbon capture rate of *P. tricornutum* was promoted by all three  $CO_2$  concentrations, which were increased by 33.4 %, 50.8 % and 149.9 % at 2 %, 5 % and 7.5 %  $CO_2$  concentrations

on average, increasing with the increase of  $CO_2$  concentration. Based on GAMs analysis, during the entire culture period at 2 %  $CO_2$  concentration, the promotion of carbon capture rate reached a maximum on day 8 (an increase of nearly 8 pg  $\operatorname{cell}^{-1} \operatorname{d}^{-1}$ ), and then weakened (Fig. 8D). The promoting effect of 5 %  $CO_2$  on carbon capture rate showed a fluctuating upward trend (Fig. 8E). The initial promoting effect of 7.5 %  $CO_2$  decreased with the extension of culture time, and there was a small increase after day 12 (Fig. 8F).

#### 3.10. Total lipid and lipid productivity at different CO<sub>2</sub> concentrations

Total lipid was increased by all high CO $_2$  concentrations, ranged from 38 %–157 % and the strongest promoting effect occurred at 5 % CO $_2$  on day 138. Although HC always showed a trend of promotion, total lipid was decreased with extension of the culture time (Fig. 9 A-C). For instance, the total lipid of AC and HC on day 8 was 16.8 % and 28.9 % respectively, while it was 6.6 % and 16.9 % on day 138 at 5 % CO $_2$  concentration (Fig. 9B). Similar trend was appeared in lipid productivity, there were significant positive effects at all CO $_2$  concentrations (ANOVA, all p < 0.05), and it was enhanced by 93.6 %, 96.9 % and 124.7 % on average at 2 % CO $_2$ , 5 % CO $_2$  and 7.5 % CO $_2$  concentration, respectively (Fig. 9D-F).

# 3.11. Fv/Fm, NPQ, and photosynthetic pigments at 7.5 % CO $_2$ & N limitation

CO<sub>2</sub>, N and time interacted on the Fv/Fm (ANOVA, all p < 0.05, Supplementary Table 3). With the prolongation of culture time, the inhibition effects of high CO<sub>2</sub> or nitrogen deficiency became increasingly intense (Fig. 10A). For instance, the inhibition rates of high CO<sub>2</sub> (HCHN) were 4.4 %, 7.1 %, 6.1 % and 10.2 % respectively at 0 h, 6 h, 12 h and 24 h (LSD, all p < 0.05) compared to ACHN. In addition, the inhibition rates of N deficiency (ACLN) were 6.3 %, 8.6 % and 16.9 % respectively at 6 h, 12 h and 24 h (LSD, all p < 0.05) compared to ACHN. The combination of high CO<sub>2</sub> and N deficiency (HCLN) led to further decrease in Fv/Fm and the inhibition rate reached the maximum of 27.4 % at 24 h (LSD, all

p < 0.05, Fig. 10A) compared to ACHN.

As for NPQ, the interaction between any two factors was significant among the three factors (CO $_2$ , N limitation and time, ANOVA, all p < 0.05, Supplementary Table 3). NPQ under all condition increased with induction time, with that under HCLN increasing most rapidly (Fig. 10B). Contrast to Fv/Fm, high CO $_2$  and N deficiency (HCLN) enhanced NPQ and their combination resulted in further increases. The highest NPQ occurred at 24 h under the combination of high CO $_2$  and N deficiency, which was 270 % higher than the control (ACHN).

The three factors had a significant interaction on Chl a content of P. tricornutum (ANOVA, p < 0.05, Supplementary Table 3). Chl a content under high CO $_2$  (HCHN) or N deficiency (ACLN) showed a pattern of first increase and then decrease with induction time while it continuously increased under the combination of high CO $_2$  and N deficiency (Fig. 10C). High CO $_2$  and N deficiency reduced Chl a content by 26.1 % and 47.3 % respectively at 24 h while their combination increased it by 36.8 % at 24 h (Fig. 10C) compared to ACHN.

The interaction effect of three factors also appeared on carotenoid content (ANOVA, p < 0.05, Supplementary Table 3). The patterns of carotenoid content under different conditions were similar to those of Chl a content (Fig. 10D). The highest carotenoid content (0.22 pg cell $^{-1}$ ) was found under HCLN at 24 h, which was 43.3 % higher than that under control (ACHN).

# 3.12. POC, carbon capture rate, total lipid and lipid productivity at 7.5 % CO<sub>2</sub> & N limitation

 $CO_2$ , N and time had an interactive effect on POC content (ANOVA, Supplementary Table 3). POC content under ambient  $CO_2$  showed a trend of first increase and then decrease with induction time while it continually increased under high  $CO_2$  (Fig. 11A). High  $CO_2$  (HCHN) significantly improved POC content by 26.5 %, 69.8 % and 80.8 % respectively at 6 h, 12 h and 24 h (LSD, all p < 0.05) compared to ACHN. Nitrogen deficiency had insignificant effects on POC at any time point. However, when high  $CO_2$  and nitrogen limitation were superimposed, the promotion effect was greater, which was 52.6 %, 77.2 % and 107.6

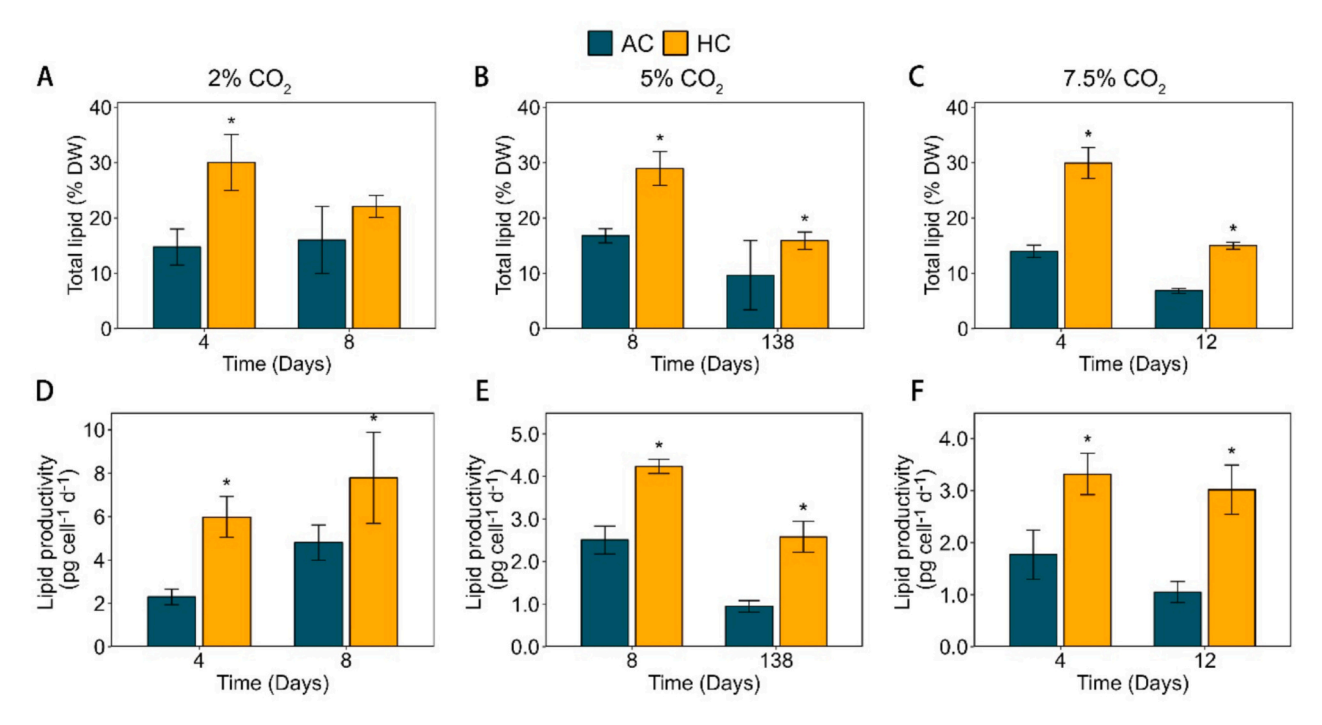


**Fig. 9.** Total lipid content (% DW) and lipid productivity of *P. tricornutum* cultured under ambient (AC) and elevated  $CO_2$  (HC) conditions. (A) and (D) for  $2 \% CO_2$ , (B) and (E) for  $5 \% CO_2$ , (C) and (F) for  $7.5 \% CO_2$ . ACHN is the control in this experiment. The value is mean  $\pm$  standard deviation (SD), and \* indicates that there is a significant difference between the HC and AC (p < 0.05).

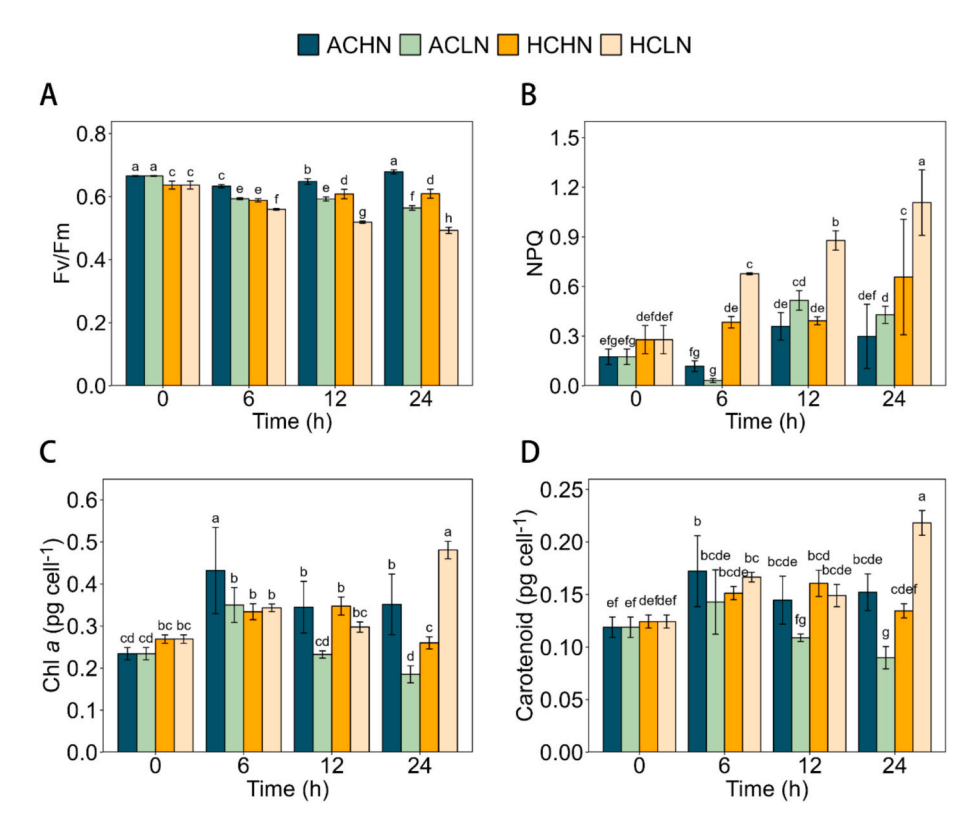


**Fig. 10.** Combined effects of high CO<sub>2</sub> concentration and nitrate deficiency on (A) Fv/Fm, (B) NPQ, (C) Chl a content and (D) carotenoid content of P. tricornutum at different induction times. AC = ambient CO<sub>2</sub> (0.04 % CO<sub>2</sub>); HC = higher CO<sub>2</sub> (7.5 % CO<sub>2</sub>); LN = lower nitrate (0 μmol mL<sup>-1</sup>); HN = higher nitrate (882.35 μmol mL<sup>-1</sup>). ACHN is the control in this experiment. The value is mean  $\pm$  standard deviation (SD), and different letters in each panel indicate that there is a significant difference between the treatments (p < 0.05).

% at 6 h, 12 h and 24 h, respectively (LSD, all p < 0.05, Fig. 11A) compared to ACHN.

 $\rm CO_2$  and interacted with time or N carbon capture rate (ANOVA, all p<0.05, Supplementary Table 3). The effect of high  $\rm CO_2$  (HCHN) changed from a positive effect at 6 h (44.7 %) to a neutral effect at 12 h, and to a negative effect at 24 h (44.4 %) for high nitrogen condition (LSD, all p<0.05, Fig. 11B) compared to ACHN. However, when cells were cultured under nitrogen deficiency (HCLN), the CO $_2$  effects were all positive and increased by 56.6 % (LSD, p<0.05), 4.9 % (LSD, p=0.059) and 108.1 % (LSD, p<0.05) respectively at 6 h, 12 h, and 24 h compared to ACLN. Moreover, the coupling of high CO $_2$  and nitrogen deficiency resulted in a synergistic promoting effect at 6 h. HCLN improved carbon capture rate by 69.1 % (LSD, p<0.05), which was 16.3 % higher than the sum of separate HC and LN effects (Fig. 11B) compared to ACHN.

The interactive effect of all three factors was significant on total lipid content (ANOVA, all p < 0.05, Supplementary Table 3). Lipid content under HN showed a trend of first increase and then decrease with induction time while it continually increased under LN (Fig. 11C). High CO<sub>2</sub> (HCHN) enhanced lipid content by 118.7 % at 0 h and 46.1 % at 6 h while the effect was insignificant at 12 h or 24 h compared to ACHN. On the contrary, the positive effect of nitrogen deficiency (HCLN) on total lipid increased with induction time from 4.7 % at 6 h, to 110.8 % at 24 h compared to HCHN. With the prolongation of culture time, the total lipid of HCLN showed an increasing trend, with the highest (20.8 % DW) occurring at 24 h (Fig. 11C).

 $\rm CO_2,~N$  and time interacted on lipid productivity (ANOVA, Supplementary Table 3). Lipid productivity under each condition decreased with induction time (Fig. 11D). Both high  $\rm CO_2$  and N deficiency enhanced lipid productivity at 6 h but their combination did not impose any significant effect. At 12 h, only N deficiency increased lipid productivity. At 24 h, there was no significant difference between any two

conditions (Fig. 11D).

#### 3.13. Fatty acid content and productivity at 7.5 % CO<sub>2</sub> & N limitation

The quality of biodiesel can be reflected by its fatty acid composition. Any two factors interacted on SFA and MUFA while a three-factor interaction on PUFA was found (ANOVA, all p < 0.05, Supplementary Table 3). High CO<sub>2</sub> (HCHN) increased the SFA content by 54.9 % (LSD, p < 0.05) at 6 h and did not significantly affect it at 12 h or 24 h under at HN compared to ACHN, while high CO<sub>2</sub> (HCLN) showed the negative effects under nitrogen deficiency condition ranged from 24.5 % to 36.5 % (Table 1) compared to ACLN. N deficiency (ACLN) enhanced SFA content under ambient CO2 by 111.4 %, 124.0 % and 290.4 % respectively at 6 h, 12 h and 24 h (LSD, all p < 0.05) while it only enhanced SFA content under high CO<sub>2</sub> by 147.9 % at 24 h compared to ACHN. High CO2 enhanced the content of monounsaturated fatty acids (MUFA) at HN by 138.4 %, 51.6 % and 97.4 % respectively at 6 h, 12 h and 24 h (LSD, all p < 0.05) while it did not affect MUFA content at LN and even reduced it at 24 h compared to 0.04 % CO2. N deficiency enhanced MUFA content regardless of CO2 level at all time points except for 6 h. Different from SFA and MUFA, high CO2 enhanced the content of polyunsaturated fatty acids (PUFA) at each N condition and timepoint (LSD, all p < 0.05). N deficiency did not affect PUFA content at 6 h but increased it at 12 h and 24 h. For each timepoint, the maximum PUFA content always occurred in the HCLN group (Table 1).

 ${\rm CO_2}$ , N and time interacted on SFA productivity (Supplementary Table 3). High  ${\rm CO_2}$  enhanced SFA productivity at HN but reduced it at LN for each timepoint (Table 2). N deficiency increased SFA productivity at AC but did not affect it at HC for each timepoint.  ${\rm CO_2}$  interacted with N or time on MUFA productivity (Supplementary Table 3). High  ${\rm CO_2}$  increased MUFA productivity at HN for each timepoint. At LN,  ${\rm CO_2}$  increased MUFA productivity at 6 h, did not affect it at 12 h and reduced

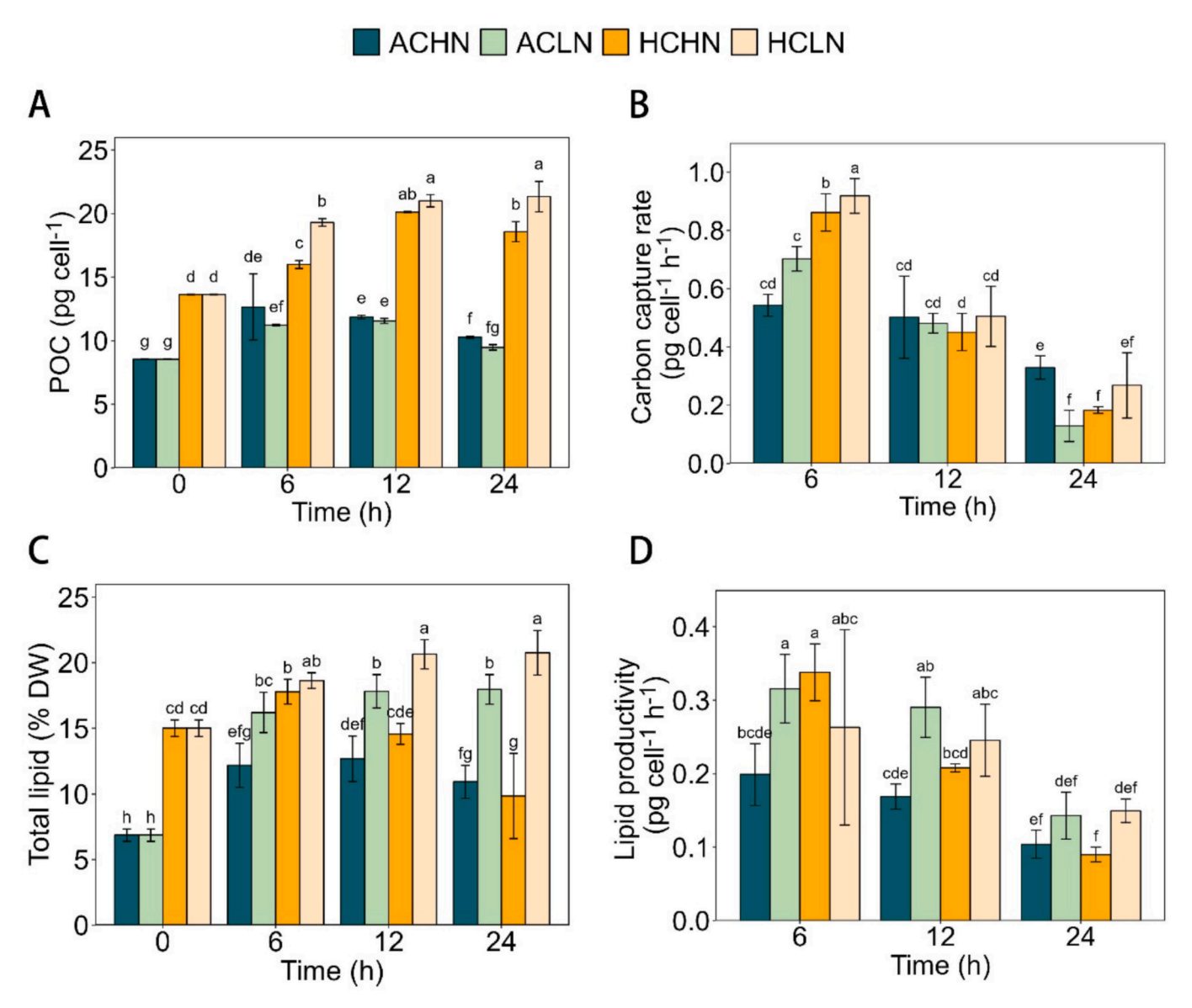


**Fig. 11.** Combined effects of high  $CO_2$  concentration and nitrate deficiency on (A) POC content, (B) carbon capture rate, (C) total lipid and (D) lipid productivity of *P. tricornutum* at different induction times.  $AC = \text{ambient } CO_2$  (0.04 %  $CO_2$ );  $HC = \text{higher } CO_2$  (7.5 %  $CO_2$ );  $LN = \text{lower nitrate } (0 \ \mu\text{mol } \text{mL}^{-1})$ ;  $HN = \text{higher nitrate } (882.35 \ \mu\text{mol } \text{mL}^{-1})$ . ACHN is the control in this experiment. The value is mean  $\pm$  standard deviation (SD), and different letters in each panel indicate that there is a significant difference between the treatments (p < 0.05).

it at 24 h. N deficiency stimulated MUFA productivity at AC but did not affect it at HC for each timepoint.  $CO_2$  interacted with time on PUFA productivity (Supplementary Table 3). High  $CO_2$  significantly increased PUFA productivity regardless of N level. The stimulative effect was weakened with induction time. The highest values for the productivity of SFA, MUFA and PUFA all appeared under HC at 6 h. (Table 2). Similar to PUFA,  $CO_2$  also interacted with time on the productivity of EPA and DHA. High  $CO_2$  significantly increased their productivity regardless of N level. The stimulative effect was weakened with induction time. The highest values for EPA and DHA productivity were also found at HC after 6 h induction.

#### 4. Discussion

# 4.1. Response of specific growth rate and cell diameter to high CO2

Due to the slow diffusion rate of dissolved  $CO_2$  in seawater, the concentration of  $CO_2$  (10–25  $\mu$ M) is lower than the half-saturation constant of ribulose-1,5-bisphosphate carboxylase/oxygenase

(Rubisco), the rate-limiting enzyme in the Calvin cycle [24,29]. To overcome these challenges, diatoms, as well as other phytoplankton in marine, evolved the carbon dioxide concentrating mechanisms (CCMs) to take up more inorganic carbon to increase the CO2 concentration around Rubisco [25]. However, the growth of P. tricornutum was still enhanced by the elevated CO<sub>2</sub> concentration (2 % CO<sub>2</sub>), which may result from down-regulated CCMs and the saved energy from that being used for growth. In contrast to the positive effect of elevated CO<sub>2</sub>, reduced pH can impose negative effects on microalgae because it can disturb the acid-base balance both at the cell surface and within cells [30]. Therefore, the specific growth rate was significantly reduced in 5 % CO2 concentration at many time points since the seawater pH was as low as 6.38. Although CO<sub>2</sub> concentrations of 1 %–10 % were commonly tested in diatoms, their maximum CO2 tolerance threshold remained uncharacterized, and different species exhibited varying tolerance ranges. Our preliminary experiment demonstrated that an abrupt increase to 7.5 % CO<sub>2</sub> inhibited the growth of P. tricornutum (Supplementary Fig. 2). Therefore, the observed pH-driven stress under sudden CO2 increases highlights the methodological advantage of stepwise

Effects of high CO<sub>2</sub> concentration and nitrate limitation on fatty acid content and productivity of *P. tricornutum* at different induction times. AC = ambient CO<sub>2</sub> (0.04 % CO<sub>2</sub>); HC = higher CO<sub>2</sub> (7.5 % CO<sub>2</sub>); LN = lower nitrate  $(0 \mu mol mL^{-1})$ ; HN = higher nitrate (882.35  $\mu mol mL^{-1}$ ). The value is mean  $\pm$  standard deviation (SD), and different letters indicate that there is a significant difference between the treatments (p < 0.05). The

detailed fatty acid content and productivity in different compositions is showed in Supplementary Table 4&5.

	FA (μg/mg DW) C20:5n3									
ACHN ACLN ACLN HCHN ACLN ACLN ACLN ACLN ACLN ACLN ACLN ACL	n3					FA productivity (fg/cell/h)	/cell/h)			
ACHN ACHN ACHN ACHN ACHN ACHN ACHN ACHN		C22:6n3	SFA	MUFA	PUFA	C20:5n3	C22:6n3	SFA	MUFA	PUFA
AGLN HCHN HCHN AGHN AGHN HCHN AGHN AGHN AGHN AGHN AGHN	$\pm \ 0.48^{\rm d}$	$0.70\pm0.02^{\rm d}$	$12.34\pm0.59^{\rm e}$	$9.91\pm0.45^{\rm e}$	$18.06\pm0.58^{\rm dh}$	$53.81\pm0.59^{\rm b}$	$2.24 \pm 0.05^{\rm de}$	$3.73\pm0.17^{\rm f}$	$8.46\pm0.27^{\rm ei}$	$7.67\pm0.08^{\rm cfik}$
HCHN HCLN ACHN ACLN HCHN HCLN ACLN ACLN	$\pm$ 0.25 <sup>d</sup>	$0.81\pm0.05^{\rm d}$	$26.09 \pm 2.47^{\mathrm{c}}$	$21.13\pm1.59^{\mathrm{cd}}$	$18.14\pm0.42^{\mathrm{bdh}}$	$51.21 \pm 6.35^{\mathrm{b}}$	$2.52\pm0.22^{\rm d}$	$7.71\pm0.51^{\rm k}$	$17.47 \pm 1.54^{\rm j}$	$7.40\pm0.89^{\mathrm{ik}}$
HCLN ACHN ACHN ACHN ACHN ACHN ACHN ACHN ACH	$\pm 1.33^{\mathrm{b}}$	$2.17 \pm 0.20^{\mathrm{b}}$	$19.12\pm0.96^{\mathrm{de}}$	$23.62 \pm 1.06^{\mathrm{c}}$	$28.33 \pm 1.87^{\rm ceg}$	$91.65 \pm 4.99^{\mathrm{a}}$	$8.93\pm0.49^{\rm a}$	$7.13\pm0.22^{8k}$	$24.62 \pm 0.98^8$	$14.65\pm0.83^{\rm d}$
ACHN ACLN HCHN HCLN ACHN ACHN	$\pm 0.25^a$	$2.41\pm0.02^{\rm a}$	$19.47\pm0.15^{\rm d}$	$24.48 \pm 0.42^{\mathrm{c}}$	$30.16\pm0.19^{\rm ceg}$	$88.14\pm12.02^{\mathrm{a}}$	$8.51\pm1.26^{\rm a}$	$6.21 \pm 0.92^{\rm ceg}$	$21.81 \pm 2.85^{\mathrm{c}}$	$13.36\pm1.89^{\mathrm{ad}}$
AGLN HCHN HCLN ACHN AGHN	$\pm 0.93^{ m d}$	$0.71\pm0.02^{\rm d}$	$14.40\pm4.65^{\mathrm{e}}$	$12.18\pm4.12^{\mathrm{e}}$	$16.29\pm1.20^{\rm dh}$	$31.30\pm0.49^{\rm cd}$	$1.48\pm0.08^{\rm e}$	$2.76\pm0.67^{\rm j}$	$6.54 \pm 1.66^{\mathrm{i}}$	$4.42\pm0.04^{\rm ghj}$
HCHN HCLN ACHN ACLN	$\pm~0.60^{\rm c}$	$0.85\pm0.03^{\rm d}$	$32.25 \pm 5.52^{\mathrm{b}}$	$27.91 \pm 4.67^{\mathrm{bc}}$	$20.37\pm0.76^{\mathrm{i}}$	$39.42 \pm 3.76^{\mathrm{c}}$	$1.83 \pm 0.18^{\mathrm{de}}$	$6.46\pm0.72^{\mathrm{eg}}$	$15.54\pm1.85^{\rm dhj}$	$5.65\pm0.52^{\rm h}$
HCLN ACHN ACLN	$16.81\pm0.16^{\mathrm{cd}}$	$1.67\pm0.01^{\rm c}$	$16.02\pm0.37^{\mathrm{de}}$	$18.47\pm0.06^{\rm d}$	$22.42\pm0.23^{\rm f}$	$47.64\pm2.68^{\mathrm{bc}}$	$4.66\pm0.27^{\rm b}$	$4.06\pm0.28^{\mathrm{bfi}}$	$13.03\pm0.70^{\rm adeh}$	$7.86\pm0.49^{\rm fik}$
ACHN		$2.10\pm0.06^{\rm b}$	$24.34 \pm 1.34^{\mathrm{cd}}$	$26.99 \pm 1.24^{\mathrm{bc}}$	$28.71\pm0.80^{\mathrm{eg}}$	$50.49\pm4.14^{\mathrm{b}}$	$4.50\pm0.34^{\rm b}$	$4.75\pm0.51^{\rm i}$	$14.65\pm1.33^{\rm h}$	$7.73\pm0.63^{\rm k}$
	$\pm 1.17^{ m d}$	$0.74\pm0.02^{\rm d}$	$10.30\pm1.50^{\mathrm{e}}$	$7.93\pm1.37^{\rm e}$	$16.65\pm1.37^{\rm h}$	$21.38 \pm 2.04^{\mathrm{d}}$	$1.04 \pm 0.06^{\mathrm{e}}$	$1.33\pm0.24^{\rm h}$	$2.87 \pm 0.59^{\rm f}$	$3.00\pm0.30^{\rm j}$
	$\pm~0.82^{\rm c}$	$0.90 \pm 0.06^{ m d}$	$40.22\pm1.65^{\rm a}$	$37.88\pm1.38^{\rm a}$	$21.76\pm0.98^{\rm fi}$	$20.06\pm1.83^{\rm d}$	$0.95\pm0.10^{\rm e}$	$3.98\pm0.25^{\rm fi}$	$10.39\pm0.65^{\mathrm{e}}$	$2.94\pm0.26^{\mathrm{gj}}$
HCHN 20.46 ± 0	$20.46 \pm 0.43^{\rm b}$	$2.15\pm0.04^{\rm b}$	$14.38\pm0.62^{\rm e}$	$15.65\pm0.57^{\rm d}$	$26.52\pm0.47^{\mathrm{ac}}$	$33.65\pm0.33^{\mathrm{cd}}$	$3.50\pm0.12^{\rm c}$	$2.11 \pm 0.08^{\rm dhj}$	$6.40\pm0.15^{\rm bi}$	$5.40\pm0.02^{\rm beh}$
HCLN $23.23 \pm 0$	$23.23 \pm 0.37^{\mathrm{ab}}$	$2.06\pm0.09^{\rm b}$	$25.54\pm2.02^{\mathrm{c}}$	$29.58\pm2.39^{\mathrm{b}}$	$29.44\pm0.48^8$	$28.16\pm0.85^{\rm d}$	$2.46\pm0.04^{\rm d}$	$2.78\pm0.25^{\rm adj}$	$8.94 \pm 0.85^{\mathrm{bei}}$	$4.41\pm0.12^{\rm eghj}$

acclimation [1,14,31]. *P. tricornutum* owns the characteristics of fast generation renewal rate and strong adaptability [32,33]. Therefore, after stepwise domestication, it showed a stronger acclimation to high  $\rm CO_2$  concentrations, and the negative effect on growth rate disappeared by the end of 5 %  $\rm CO_2$  culture and during 7.5 %  $\rm CO_2$  culture compared to 0.04 %  $\rm CO_2$ . High  $\rm CO_2$  concentrations might have altered the residence time of each phase of the cell cycle, for instance, increasing the residence time of the G1 phase made it easier to observe larger cell diameter at the same time every day. And the increased cell diameter might provide preparation for the accumulation of carbon and lipids, fatty acids, etc.

### 4.2. Response of photosynthesis and carbon assimilation to high CO2

High CO2 could enhance photosynthesis, which was manifested in the increase of Fv/Fm [34]. Given the high CO<sub>2</sub> concentrations of 800-1000 ppm in previous studies [34,35], the positive effects of increased CO2 may dominate. In our study, high CO2 was set to well above 1000 ppm (2-7.5 % CO<sub>2</sub>), so the negative effects of pH reduction dominated, resulting in Fv/Fm reduction in photosynthesis. In addition, higher energy dissipation (NPQ) is usually induced when cells suffer from environmental stress [36,37], and elevated NPO at high CO<sub>2</sub> concentrations (2–7.5 %) in this study also supports this conclusion. As CO<sub>2</sub> concentration increased from 5 % to 7.5 %, P. tricornutum began to activate their self-protection mechanisms to resist environmental stress by synthesizing more pigments. The increased content of Chl a could increase the rate of light energy absorption and transfer in microalgae photosynthesis, increase the rate of light reaction and synthesize more ATP and NADPH [38,39]. Studies had shown that high CO<sub>2</sub> levels could increase the sensitivity of algae to high light intensity, and increasing carotenoid content could help reduce the occurrence of light inhibition of *P. tricornutum* [40,41]. The increase of light-harvesting pigments was conducive to the photoreaction process of photosynthesis, and thus to the enhancement of the carbon fixation process in the dark reaction [42]. Therefore, high CO2 increased carbon assimilation (indexed by POC content) of P. tricornutum at all three high CO<sub>2</sub> levels. The increased particulate organic carbon resulted in increased carbon capture rate of P. tricornutum cultured under the three high CO<sub>2</sub> levels (33.4 %-149.9 %), which could improve the degree of carbon capture and reduce CO2 emission from industrial waste gases [14]. After the stepwise domestication from 2 % to 7.5 % CO2 concentration, it was found that both carbon assimilation and carbon capture rates were highest at 7.5 % CO<sub>2</sub>, which might be related to the trends of photosynthesis and pigments.

When nitrogen was deficient, the overall trends of photosynthesis, pigment contents and carbon assimilation of *P. tricornutum* were consistent with those mentioned above, except for carbon capture rate. The inhibitory effect of nitrogen deficiency on growth became more obvious with the prolongation of culture time, which indirectly affected the contribution of *P. tricornutum* to carbon capture. Therefore, after weighing various parameters, it is particularly important to choose a suitable culture time of *P. tricornutum* to achieve the maximum carbon capture.

# 4.3. Increased total lipid and lipid productivity by high ${\rm CO}_2$

The necessary conditions for lipid biosynthesis are ATP and carbon skeleton, which depend on light and dark reactions of photosynthesis [7,15]. Previous studies have shown that enhanced photosynthesis by increasing  $\rm CO_2$  concentrations could improve lipid synthesis. For instance, the lipid content of S. costatum was enhanced by 87 % at 10 %  $\rm CO_2$  concentration compared to 0.04 %  $\rm CO_2$  concentration [1]. In this study, 5 % and 7.5 %  $\rm CO_2$  stimulated lipid content of P. tricornutum by 96 % and 157 %, respectively, showing a greater enhancement compared to S. costatum (26.8–87 %). However, the Fv/Fm of P. tricornutum was slightly reduced by high  $\rm CO_2$  concentration. Therefore, for P. tricornutum, the increased lipid content could not be attributed to photosynthesis but rather to enhanced provision of intracellular

carbon skeletons. In simple terms, diatoms uptake dissolved inorganic carbon (DIC, including CO2 and HCO3) from seawater via passive diffusion or active transport. HCO<sub>3</sub> is then converted to CO<sub>2</sub> by carbonic anhydrase (CA) for use in the dark reactions (Calvin cycle), which is powered by ATP and NADPH generated in the photosynthesis. To compensate for the high  $CO_2$  half-saturation constant ( $K_m$ , 23–68  $\mu$ mol L<sup>-1</sup>) of Rubisco, the key rate-limiting enzyme in the Calvin cycle for carbon fixation, diatoms activate their CCMs. During the Calvin cycle, CO2 is fixed into 3-phosphoglycerate (3-PGA) and subsequently reduced to glyceraldehyde-3-phosphate (G3P), which involved in glycolysis to produce pyruvate. Subsequently, pyruvate is converted into acetyl-CoA—a key precursor for lipid biosynthesis—catalyzed by pyruvate dehydrogenase [18-21]. With the increasing of CO<sub>2</sub> concentration, the Rubisco carboxylation activity could be stimulated, promoting carbon fixation and subsequently elevating the production of lipid precursors such as acetyl-CoA. Therefore, high CO2 can provide an abundant carbon source for lipid biosynthesis [18]. And the increased cell size and POC content also contributed to lipid accumulation in cells.

In addition to lipid content, lipid productivity is also a key index for biodiesel production [7,43], as it relates to the maximum economic benefit. At 2 %  $\rm CO_2$  concentration, enhanced lipid productivity can be attributed to both increased specific growth rate and POC content. Although the growth rate of *P. tricornutum* was decreased at 5 %  $\rm CO_2$  concentration, lipid productivity was still increased, which could result from a 96 % increase in POC content. As *P. tricornutum* gradually acclimated to high  $\rm CO_2$  concentrations, the promoting effect on lipid productivity reached a maximum (116 %) at 7.5 %  $\rm CO_2$  concentration compared to control. Therefore, after the gradual domestication of *P. tricornutum*, more lipid content and higher lipid productivity will be obtained, which not only saves economic costs but also helps algae to absorb more  $\rm CO_2$ .

To improve lipid content and productivity, nitrogen limitation is usually adopted to culture algae because nitrogen has been found to be a critical factor that affects lipid content [7]. The results of the acclimation experiments indicate that increasing cell size contributed to the increase in lipid content of each cell under high CO2 concentrations. When nitrogen was limited, algae could still synthesize lipids, although the rate of cell division decreases, so more lipids would be accumulated in algae [30]. When high CO<sub>2</sub> was coupled with nitrogen deficiency, the positive effects of them on lipids and lipid productivity could be synergistic. In this study, the synergistic effect was clearly observed in terms of lipid content that had the highest value under the condition of high CO2 and N deficiency. And for lipid productivity, the promoting effects of high CO<sub>2</sub> and N deficiency decreased with the culture time. The combination of high CO2 and N deficiency did not result in further increase in lipid productivity, which could be attributed to the negative effect of nitrogen deficiency on growth. Therefore, for economic cost and time cost considerations, in order to obtain more lipids and higher lipid production at the same time, we recommend that the induction time be controlled between 6 and 12 h in future industrial production.

#### 4.4. Effects of 7.5 % CO2 & N limitation on fatty acids

The content and proportion of different types of fatty acids affect the quality of biodiesel. Long chain SFA and MUFA have a positive effect on the oxidation stability of biodiesel, but PUFA has a negative effect on the oxidation stability as bisallylic hydrogens are susceptible to free radical attack [7]. The effects of nitrogen limitation and high CO<sub>2</sub> on fatty acid compositions have been widely reported. For example, the proportions of SFA and MUFA were increased, and PUFA was decreased in *P. tricornutum* [44], *S. menzelii* SM-2 [15] and *S. costatum* [7] under N limitation. And high CO<sub>2</sub> increased MUFA and PUFA but decreased SFA in *S. costatum*, *S. obliquus* and *C. pyrenoidosa* [1,45]. However, the study indicated that within 12 h after CO<sub>2</sub> and nitrogen deficiency coupling, the proportion of SFA and PUFA only decreased slightly, ranging from 2.13 % to 4.34 %, while the proportion of MUFA increased by 5.31 % to

8.45 %. In addition, the productivity promotion extents of MUFA and PUFA were higher than that of SFA productivity, which indicated that HCLN not only had a slight effect on the quality of P. tricornutum biodiesel, but also greatly improved the productivity and saved the production cost, especially for unsaturated fatty acids at 6 h of culture. In addition, HCLN also significantly promoted the accumulation of lipid contents. Under environmental stress, particularly under nitrogen deficiency, protein synthesis was halted, redirecting intracellular carbon flux from protein production toward the synthesis of either lipid or carbohydrate [30]. Compared to carbohydrates, lipid and fatty acids exhibit higher energy density, making them the preferred biosynthetic products for fueling post-stress cellular recovery and reconstruction [30,46]. However, this energy conservation strategy can lead to tradeoffs between lipids and cellular components. For instance, lightharvesting components (such as photosynthetic pigments) and related physiological performance (e.g., Fv/Fm) were reduced in this study to meet the material and energy demand of lipid synthesis. Meanwhile, HC environments can supply adequate carbon skeleton for lipid synthesis, potentially enhancing lipid content in microalgae [47]. Previous studies have demonstrated that both high CO2 and nitrogen limitation significantly upregulated enzymes associated with lipid and fatty acid synthesis, such as acetyl-CoA carboxylase—the first rate-limiting enzyme in fatty acid biosynthesis, which was benefit to increase in lipid and fatty acid accumulation in microalgae [48-50]. Therefore, different environmental pressures can induce microalgae to produce different fatty acid compositions and productivity, which provides guiding suggestions for the future production of different types of fatty acids by microalgae.

PUFA contains two fatty acids that are crucial for aquaculture and human health, namely eicosapentaenoic acid (EPA) and docosahexaenoic acid (DHA) [51]. As global demand for omega-3 fatty acids grows, researchers are increasingly focusing on microalgae-recognized as highly productive and sustainable sources of EPA and DHA for commercial production [52,53]. Here, we present an innovative, ecofriendly strategy to enhance EPA and DHA biosynthesis in P. tricornutum under combined stress of hypercapnia (high CO2) and nitrogen (N) limitation. Our findings demonstrate that dual stress conditions significantly elevated both EPA/DHA content and productivity. Specifically, at 6-, 12-, and 24-h time points, the promotion effect diminished over culture duration—with the notable exception of EPA content, which remained stable (59-64 %). Optimization analysis revealed that the 6-h cultivation period yielded optimal results compared to control: EPA content (59 % increase) and productivity (64 % increase), alongside DHA content (246 % increase) and productivity (280 % increase). The promoting effects of high CO2 on EPA and DHA were stronger than those occurring in EPA (18.4 %) and DHA (74.2 %) content of S. costatum under non-nitrogen-limited condition [1]. These outcomes represent substantial improvements over baseline metrics. This study establishes a novel, cost-effective protocol for scalable production of omega-3 fatty acids, addressing both commercial demands and environmental imperatives. For instance, a key advantage of marine microalgae over freshwater species lies in their innate salt tolerance. Seawater-based cultivation circumvents freshwater dependency and generates synergistic sustainability gains by alleviating pressure on dwindling freshwater supplies [54,55]. More importantly, for industrialscale production, both high concentration CO2 and nitrogen limited conditions can be readily achieved without substantial additional costs, which makes marine microalgae cultivation using industrial flue gas more economical, significantly reducing production expenses [56,57]. Furthermore, existing EPA/DHA production technologies have reached considerable maturity, combined with their high values and market demands, providing both technical feasibility and economic justification for microalgae-derived EPA/DHA manufacturing [58-60]. Notably, industrial flue gases comprise multiple components besides CO<sub>2</sub>. Prior to large-scale algal cultivation, these non-CO<sub>2</sub> gases must be removed—a process that simultaneously enables their recovery and potential reuse in other industrial applications. By leveraging microalgal stress

physiology, we achieve rapid biosynthesis under resource-efficient conditions, positioning *P. tricornutum* as a promising chassis for sustainable aquaculture feed and nutraceutical production.

#### 5. Conclusion

In this study, the model of stepwise CO2 acclimation (2 %-7.5 % CO<sub>2</sub>) was firstly employed to obtain optimal lipid and fatty acid productivity from P. tricornutum. Following acclimation, P. tricornutum demonstrated exceptional carbon capture rate and lipid production capacity. The coupling of nitrogen limitation and high CO2 further enhanced lipid accumulation and biodiesel productivity. The levels of valuable polyunsaturated fatty acids (PUFAs), including DHA and EPA, were also enriched. These findings indicate that the stepwise CO2 acclimation strategy is an effective approach for achieving simultaneous CO2 mitigation and high-value product synthesis using microalgae. While P. tricornutum has been proved effective for CO<sub>2</sub> capture and PUFA production, further research is needed to evaluate the universality and scalability of this approach across a broader range of microalgal species. Moreover, substantial mechanistic investigations remain to be explored. For instance, identification of key regulatory genes governing microalgal adaptation to industrial waste gas, and potential development of CRISPR-engineered strains with enhanced CO2 resilience. Beyond nitrogen limitation, identifying additional factors that can enhance microalgal lipid and fatty acid biosynthesis will be critical to optimizing carbon capture and utilization efficiencies. Such studies would provide critical insights into the potential for large-scale industrial applications.

#### CRediT authorship contribution statement

Shuyu Xie: Writing – review & editing, Validation, Methodology, Investigation, Formal analysis. Xin Zhao: Writing – review & editing, Writing – original draft, Validation, Methodology, Formal analysis. Yuan Feng: Writing – review & editing, Validation, Methodology, Investigation. Guang Gao: Writing – review & editing, Validation, Supervision, Methodology, Funding acquisition, Formal analysis, Conceptualization.

#### Declaration of competing interest

The authors declare that they have no known competing financial interests or personal relationships that could have appeared to influence the work reported in this paper.

#### Acknowledgments

This work was supported by the National Key Research and Development Program of China (2022YFC3105304), the National Natural Science Foundation of China (42576209), the Open Foundation of Key Laboratory of Marine Environmental Survey Technology and Application, Ministry of Natural Resources (MESTA-2024-A001), the International Cooperation Seed Funding Project for China's Ocean Decade Actions (GHZZ3702840002024020000020), XIAMEN UNIVERSITY PINGTAN INSTITUTE (XMUPTI2024001, XMUPTI2024002), and Ocean Negative Carbon Emissions (ONCE) program.

# Appendix A. Supplementary data

Supplementary data to this article can be found online at  $\frac{https:}{doi.}$  org/10.1016/j.algal.2025.104298.

# Data availability

Data will be made available on request.

#### References

- [1] M. Wu, G. Gao, Y. Jian, J. Xu, High CO<sub>2</sub> increases lipid and polyunsaturated fatty acid productivity of the marine diatom *Skeletonema costatum* in a two-stage model, J. Appl. Phycol. 34 (2021) 43–50, https://doi.org/10.1007/s10811-021-02619-5.
- [2] T.A. Jacobson, J.S. Kler, M.T. Hernke, R.K. Braun, K.C. Meyer, W.E. Funk, Direct human health risks of increased atmospheric carbon dioxide, Nat. Sustain. 2 (2019) 691–701, https://doi.org/10.1038/s41893-019-0323-1.
- [3] S.A. Razzak, S.A.M. Ali, M.M. Hossain, H. deLasa, Biological CO<sub>2</sub> fixation with production of microalgae in wastewater – a review, Renew. Sust. Energy Rev. 76 (2017) 379–390, https://doi.org/10.1016/j.rser.2017.02.038.
- [4] H.M. Singh, R. Kothari, R. Gupta, V.V. Tyagi, Bio-fixation of flue gas from thermal power plants with algal biomass: overview and research perspectives, J. Environ. Manage. 245 (2019) 519–539, https://doi.org/10.1016/j.jenvman.2019.01.043.
- [5] W.V. Reid, M.K. Ali, C.B. Field, The future of bioenergy, Glob. Chang. Biol. 26 (2019) 274–286, https://doi.org/10.1111/gcb.14883.
- [6] B. Subhadra, M. Edwards, An integrated renewable energy park approach for algal biofuel production in United States, Energy Policy 38 (2010) 4897–4902, https:// doi.org/10.1016/j.enpol.2010.04.036.
- [7] G. Gao, M. Wu, Q. Fu, X. Li, J. Xu, A two-stage model with nitrogen and silicon limitation enhances lipid productivity and biodiesel features of the marine bloomforming diatom *Skeletonema costatum*, Bioresour. Technol. 289 (2019) 121717, https://doi.org/10.1016/j.biortech.2019.121717.
- [8] K. Ullah, M. Ahmad, Sofia, V.K. Sharma, P. Lu, A. Harvey, M. Zafar, S. Sultana, Assessing the potential of algal biomass opportunities for bioenergy industry: a review, Fuel 143 (2015) 414–423, https://doi.org/10.1016/j.fuel.2014.10.064.
- [9] O.M. Adeniyi, U. Azimov, A. Burluka, Algae biofuel: current status and future applications, Renew. Sust. Energy Rev. 90 (2018) 316–335, https://doi.org/ 10.1016/j.rser.2018.03.067.
- [10] G. Gao, J. Beardall, M. Bao, C. Wang, W. Ren, J. Xu, Ocean acidification and nutrient limitation synergistically reduce growth and photosynthetic performances of a green tide alga *Ulva linza*, Biogeosciences 15 (2018) 3409–3420, https://doi. org/10.5194/bg-15-3409-2018.
- [11] G. Gao, J. Burgess, M. Wu, S. Wang, k. Gao, Using macroalgae as biofuel: current opportunities and challenges, Bot. Mar. 63 (2020) 355–370, https://doi.org/ 10.1515/bot-2019-0065
- [12] S. Dickinson, M. Mientus, D. Frey, A. Amini-Hajibashi, S. Ozturk, F. Shaikh, D. Sengupta, M.M. El-Halwagi, A review of biodiesel production from microalgae, Clean Technol. Environ. Policy 19 (2017) 637–668, https://doi.org/10.1007/ s10098-016-1309-6.
- [13] L. Peng, D. Fu, H. Chu, H. Qi, Biofuel production from microalgae: a review, Environ. Chem. Lett. 18 (2020) 285–297, https://doi.org/10.1007/s10311-019-00939-0.
- [14] S. Xie, F. Lin, X. Zhao, G. Gao, Enhanced lipid productivity coupled with carbon and nitrogen removal of the diatom *Skeletonema costatum* cultured in the high CO<sub>2</sub> level, Algal Res. 61 (2022) 102589, https://doi.org/10.1016/j.algal.2021.102589.
- [15] X. Jiang, Q. Han, X. Gao, G. Gao, Conditions optimising on the yield of biomass, total lipid, and valuable fatty acids in two strains of *Skeletonema menzelii*, Food Chem. 194 (2016) 723–732, https://doi.org/10.1016/j.foodchem.2015.08.073.
- [16] R.K. Saini, Y.-S. Keum, Omega-3 and omega-6 polyunsaturated fatty acids: dietary sources, metabolism, and significance — a review, Life Sci. 203 (2018) 255–267, https://doi.org/10.1016/j.lfs.2018.04.049.
- [17] T.C. Adarme-Vega, K.Y.D. Lim, M. Timmins, F. Vernen, Y. Li, M.P. Schenk, Microalgal biofactories: a promising approach towards sustainable omega-3 fatty acid production, Microb. Cell Fact. 11 (2012) 96, https://doi.org/10.1186/1475-2850-11-96
- [18] J.N. Young, B.M. Hopkinson, The potential for co-evolution of CO<sub>2</sub>-concentrating mechanisms and Rubisco in diatoms, J. Exp. Bot. 68 (2017) 3751–3762, https://doi.org/10.1093/jxb/erx130.
- [19] A. Gruber, T. Weber, C.R. Bártulos, S. Vugrinec, P.G. Kroth, Intracellular distribution of the reductive and oxidativepentose phosphate pathways in two diatoms, J. Basic Microb. 49 (2009) 58–72, https://doi.org/10.1002/ johm 200800339
- [20] Y.Q. Li, H. Xu, F.X. Han, J.X. Mu, D. Chen, B. Feng, H.Y. Zeng, Regulation of lipid metabolism in the green microalga *Chlorella protothecoides* by heterotrophyphotoinduction cultivation regime, Bioresour. Technol. 192 (2015) 781–791, https://doi.org/10.1016/j.biortech.2014.07.028
- [21] D. Chen, X. Yuan, L.M. Liang, K. Liu, H.Y. Ye, Z.Y. Liu, Y.F. Liu, L.Q. Huang, W. J. He, Y.Q. Chen, Y.D. Zhang, T. Xue, Overexpression of acetyl-CoA carboxylase increases fatty acid production in the green alga Chlamydomonas reinhardtii, Biotechnol. Lett. 41 (2019) 1133–1145, https://doi.org/10.1007/s10529-019-02715-0.
- [22] V. Singh, A. Tiwari, M. Das, Phyco-remediation of industrial waste-water and flue gases with algal-diesel engenderment from micro-algae: a review, Fuel 173 (2016) 90–97, https://doi.org/10.1016/j.fuel.2016.01.031.
- [23] O.P. Ward, W. Yongmanitchai, Growth of and Omega-3 fatty acid production by Phaeodactylum tricornutum under different culture conditions, Appl. Environ. Microbiol. 57 (1991) 419–425, https://doi.org/10.1128/AEM.57.2.419-425.1991.
- [24] J.N. Young, A.M.C. Heureux, R.E. Sharwood, R.E.M. Rickaby, F.M.M. Morel, S. M. Whitney, Large variation in the Rubisco kinetics of diatoms reveals diversity among their carbon-concentrating mechanisms, J. Exp. Bot. 67 (2016) 3445–3456, https://doi.org/10.1093/jkb/erw163.
- [25] C. Shen, C.L. Dupont, B.M. Hopkinson, The diversity of CO<sub>2</sub>-concentrating mechanisms in marine diatoms as inferred from their genetic content, J. Exp. Bot. 68 (2017) 3937–3948, https://doi.org/10.1093/jxb/erx163.

- [26] M. Kitajima, W.L. Butler, Quenching of chlorophyll fluorescence and primary photochemistry in chloroplasts by dibromothymoquinone 376 (1975) 105–115, https://doi.org/10.1016/0005-2728(75)90209-1.
- [27] W. Bilger, O. Bjorkman, Role of the xanthophyll cycle in photoprotection elucidated by measurements of light-induced absorbance changes, fluorescence and photosynthesis in leaves of *Hedera canariensis*, Photosynth. Res. 25 (1990) 173–185, https://doi.org/10.1007/BF00033159.
- [28] G. Gao, K. Gao, M. Giordano, Responses to solar UV radiation of the diatom Skeletonema costatum (Bacillariophyceae) grown at different Zn<sup>2+</sup> concentrations, J. Phycol. 49 (2009) 119–129, https://doi.org/10.1111/j.1529-8817.2008.00616.
- [29] A.J. Boller, P.J. Thomas, C.M. Cavanaugh, K.M. Scott, Isotopic discrimination and kinetic parameters of RubisCO from the marine bloom-forming diatom, Skeletonema costatum, Geobiology 13 (2014) 33–43, https://doi.org/10.1111/ gbi.12112.
- [30] G. Gao, J. Xia, J. Yu, X. Zeng, Physiological response of a red tide alga (Skeletonema costatum) to nitrate enrichment, with special reference to inorganic carbon acquisition, Mar. Environ. Res. 133 (2018) 15–23, https://doi.org/10.1016/j.marenvres.2017.11.003.
- [31] A. Sabia, E. Clavero, S. Pancaldi, J.S. Rovira, Effect of different CO<sub>2</sub> concentrations on biomass, pigment content, and lipid production of the marine diatom *Thalassiosira pseudonana*, Appl. Microbiol. Biot. 102 (2018) 1945–1954, https:// doi.org/10.1007/s00253-017-8728-0.
- [32] B. Koletzko, C.C.M. Boey, C. Campoy, S.E. Carlson, N. Chang, M.A. Guillermo-Tuazon, S. Joshi, C. Prell, S.H. Quak, D.R. Sjarif, Y. Su, S. Supapannachart, Y. Yamashiro, S.J.M. Osendarp, Current information and Asian perspectives on long-chain polyunsaturated fatty acids in pregnancy, lactation, and infancy: systematic review and practice recommendations from an early nutrition academy workshop, Ann. Nutr. Metab. 65 (2014) 49–80, https://doi.org/10.1159/000365767
- [33] J. Milano, H.C. Ong, H.H. Masjuki, W.T. Chong, M.K. Lam, P.K. Loh, V. Vellayan, Microalgae biofuels as an alternative to fossil fuel for power generation, Renew. Sustain Energy Rev. 58 (2016) 180–197, https://doi.org/10.1016/j. rser.2015.12.150.
- [34] L. Qu, D.A. Campbell, K. Gao, Ocean acidification interacts with growth light to suppress CO<sub>2</sub> acquisition efficiency and enhance mitochondrial respiration in a coastal diatom, Mar. Pollut. Bull. 163 (2021) 112008, https://doi.org/10.1016/j. marpolbul.2021.112008.
- [35] S. Hu, Y. Wang, Y. Wang, Y. Zhao, X. Zhang, Y. Zhang, M. Jiang, X. Tang, Effects of elevated pCO<sub>2</sub> on physiological performance of marine microalgae *Dunaliella salina* (Chlorophyta, Chlorophyceae), J. Oceanol. Limnol. 36 (2017) 317–328, https:// doi.org/10.1007/s00343-018-6278-7.
- [36] C. Hoppe J.M., C. Hassler .S., C. Payne .D., P. Tortell .D., B. Rost, S. Trimborn, Iron limitation Modulates Ocean acidification effects on Southern Ocean phytoplankton communities, PloS One 8 (2013) e79890, https://doi.org/10.1371/journal. pone.0079890.
- [37] F.L. Figueroa, J. Bonomi-Barufi, P.S.M. Celis-Plá, U. Nitschke, F. Arenas, S. Connan, M.H. Abreu, E.-J. Malta, R. Conde-Álvarez, F. Chow, M.T. Mata, O. Meyerhoff, D. Robledo, D.B. Stengel, H. Küpper, Short-term effects of increased CO<sub>2</sub>, nitrate and temperature on photosynthetic activity in *Ulva rigida* (Chlorophyta) estimated by different pulse amplitude modulated fluorometers and oxygen evolution, J. Exp. Bot. 72 (2021) 491–509, https://doi.org/10.1093/jxb/eraa473.
- [38] J.A.L. Goldman, M.L. Bender, F.M.M. Morel, The effects of pH and pCO<sub>2</sub> on photosynthesis and respiration in the diatom *Thalassiosira weissflogii*, Photosynth. Res. 132 (2017) 83–93, https://doi.org/10.1007/s11120-016-0330-2.
- [39] S. Thangaraj, J. Sun, Transcriptomic reprogramming of the oceanic diatom skeletonema dohrnii under warming ocean and acidification, Environ. Microbiol. 23 (2020) 980–995, https://doi.org/10.1111/1462-2920.1524.
   [40] W. Li, T. Wang, D.A. Campbell, K. Gao, Ocean acidification interacts with variable
- [40] W. Li, T. Wang, D.A. Campbell, K. Gao, Ocean acidification interacts with variable light to decrease growth but increase particulate organic nitrogen production in a diatom, Mar. Environ. Res. 160 (2020) 104965, https://doi.org/10.1016/j. marenyres.2020.104965.
- [41] S. Lin, G. Gao, Y. Liu, X. Li, Z. Feng, J. Xu, An ocean acidification acclimatised green tide alga is robust to changes of seawater carbon chemistry but vulnerable to light stress, PloS One 11 (2016) e0169040, https://doi.org/10.1371/journal. pone.0169040.
- [42] B. Wang, J. Jia, Photoprotection mechanisms of Nannochloropsis oceanica in response to light stress, Algal Res. 46 (2020) 101784, https://doi.org/10.1016/j. algal.2019.101784.

- [43] M.J. Griffiths, S.T.L. Harrison, Lipid productivity as a key characteristic for choosing algal species for biodiesel production, J. Appl. Phycol. 21 (2009) 493–507, https://doi.org/10.1007/s10811-008-9392-7.
- [44] Z. Yang, P.K. Wong, C.M. Vong, J. Zhong, J. Liang, Simultaneous-fault diagnosis of gas turbine generator systems using a pairwise-coupled probabilistic classifier, Math. Probl. Eng. 2013 (2013) 1–14, https://doi.org/10.1155/2013/827128.
- [45] D. Tang, W. Han, P. Li, X. Miao, J. Zhong, CO<sub>2</sub> biofixation and fatty acid composition of *Scenedesmus obliquus* and *Chlorella pyrenoidosa* in response to different CO<sub>2</sub> levels, Bioresour. Technol. 102 (2011) 3071–3076, https://doi.org/ 10.1016/j.biortech.2010.10.047.
- [46] L. Rodolfi, G. Chini Zittelli, N. Bassi, G. Padovani, N. Biondi, G. Bonini, M. R. Tredici, Microalgae for oil: strain selection, induction of lipid synthesis and outdoor mass cultivation in a low-cost photobioreactor, Biotechnol. Bioeng. 102 (2009) 100–112, https://doi.org/10.1002/bit.22033.
- [47] Y. Feng, J. Ge, P.L. Show, C. Song, L. Wu, Z. Ma, G. Gao, Using high CO2 concentrations to culture microalgae for lipid and fatty acid production: synthesis based on a meta-analysis, Aquaculture 594 (2025) 741386, https://doi.org/10.1016/j.aquaculture.2024.741386.
- [48] S. Thangarag, J. Sun, The biotechnological potential of the marine diatom Skeletonema dohrnii to the elevated temperature and pCO2, Mar. Drugs 18 (2020) 259, https://doi.org/10.3390/md18050259.
- [49] J. Li, K.H. Pan, X.X. Tang, Y. Li, B.H. Zhu, Y. Zhao, The molecular mechanisms of Chlorella sp. responding to high CO2: a study based on comparative transcriptome analysis between strains with high- and low-CO2 tolerance, Sci. Total Environ. 763 (2021) 144185, https://doi.org/10.1016/j.scitotenv.2020.144185.
- [50] D.Y. Hou, X.T. Mao, S. Gu, H.Y. Li, J.S. Liu, W.D. Yang, Systems-level analysis of metabolic mechanism following nitrogen limitation in benthic dinoflagellate *Procentrum lima*, Algal Res. 33 (2018) 389–398, https://doi.org/10.1016/j. algal 2018 06 004
- [51] M.S. Chauton, K.I. Reitan, N.H. Norsker, R. Tveterås, H.T. Kleivdal, A technoeconomic analysis of industrial production of marine microalgae as a source of EPA and DHA-rich raw material for aquafeed: research challenges and possibilities, Aquaculture 436 (2015) 95–103, https://doi.org/10.1016/j. aquaculture.2014.10.038.
- [52] H. Jiang, K. Gao, Effects of lowering temperature during culture on the production of polyunsaturated fatty acids in the marine diatom *Phaeodactylum tricornutum* (Bacillariophyceae), J. Phycol. 40 (2004) 651–654, https://doi.org/10.1111/ i.1529-8817.2004.03112.x.
- [53] M.C. Cerón-García, J.M. Fernández-Sevilla, A. Sánchez-Mirón, F. García-Camacho, A. Contreras-Gómez, E. Molina-Grima, Mixotrophic growth of *Phaeodactylum tricornutum* on fructose and glycerol in fed-batch and semi-continuous modes, Bioresour. Technol. 147 (2013) 569–576, https://doi.org/10.1016/j.biortech.2013.08.092.
- [54] M. Shankar, P.K. Chhotaray, A. Agrawal, R.L. Gardas, K. Tamilarasan, M. Rajesh, Protic ionic liquid-assisted cell disruption and lipid extraction from fresh water Chlorella and Chlorococcum microalgae, Algal Res. 25 (2017) 228–236, https://doi. org/10.1016/j.algal.2017.05.009.
- [55] A. Widjaja, C.C. Chien, Y.H. Ju, Study of increasing lipid production from fresh water microalgae *Chlorella vulgaris*, J. Taiwan Inst. Chem E 2009 (40) (2009) 13–20, https://doi.org/10.1016/j.jtice.2008.07.007.
- Y. Zhang, S. Soldatov, I. Papachristou, N. Nazarova, G. Link, W. Frey, A. Silve, Pulsed microwave pretreatment of fresh microalgae for enhanced lipid extraction, Energy 248 (2022) 123555, https://doi.org/10.1016/j.energy.2022.123555.
   A.E.F. Abomohra, M. Wartin, M. El-Sheekh, D. Hanelt, Lipid and total fatty acid
- [57] A.E.F. Abomohra, M. Wartin, M. El-Sheekh, D. Hanelt, Lipid and total fatty acid productivity in photoautotrophic fresh water microalgae: screening studies towards biodiesel production, J. Appl. Phycol. 25 (2013) 931–936, https://doi. org/10.1007/s10811-012-9917-y.
- [58] J.T. Cui, X.M. Jiang, W.M. Zhang, C. Li, J. Gao, Positional characterization of DHA/EPA in triacylglycerol and phospholipid and production of DHA/EPA-rich phospholipid, J. Food Compos. Anal. 129 (2024) 106085, https://doi.org/10.1016/j.ifca.2024.106085.
- [59] M.K. Paidi, A. Attupuram, K.S. Udata, S.K. Mandal, Acetone diethyl ether-based biorefinery process for co-extraction of fucoxanthin, chlorophyll, DHA, and EPA from the diatom *Thalassiosira lundiana*, Algal Res. 74 (2023) 103215, https://doi. org/10.1016/j.algal.2023.103215.
- [60] L. Archer, D. Mc Gee, A. Paskuliakova, G.R. McCoy, T. Smyth, E. Gillespie, N. Touzet, Fatty acid profiling of new Irish microalgal isolates producing the highvalue metabolites EPA and DHA, Algal Res. 44 (2019) 101671, https://doi.org/ 10.1016/j.algal.2019.101671.